THE USE OF DRONES AND THERMAL CAMERA IMAGING TECHNOLOGY FOR AVIAN NEST SEARCHING

by

Roald Stander

A Thesis submitted to the Faculty of Graduate Studies of

The University of Manitoba

in partial fulfilment of the requirements of the degree of

MASTER OF ENVIRONMENT

Department of Environment and Geography

University of Manitoba

Winnipeg

ABSTRACT

In the rapidly evolving field of drone wildlife surveys, we test a commercially available drone and thermal camera as a nest searching tool for various upland nesting gamebird and non-gamebird species by evaluating the method in a multi-species, multi-habitat comparison across North America. Furthermore, the study compares the efficacy of a thermal drone system to the chain-drag method to search for upland nesting waterfowl in the Prairie Pothole Region. We also examine how factors, such as meteorology, influence thermal drone detection. This study searches for nests in four U.S. states and one Canadian province between 15 May–17 June 2017 and 8 May to 15 June 2018. We used a modified point count and automated flight line transect sampling methodologies for drone nest searching with real-time visual detection of thermal targets. We found 18 out of 22 known nests in the multi-species, multi-habitat component and identified several challenges associated with the method, such as high commission errors (60 – 95%) that impede detection. In comparing nest searching methods, we find 150 upland waterfowl nests and use a Huggins Closed Capture model to compare detection rates. We found that drone and chain drag methods have detection rates of 0.36±0.04 and 0.55±0.06, respectively. In addition, we found that the drone method has challenges detecting laying stage nests and hypothesize that the survey timing impedes their detection due to biological reasons. Finally, we considered various factors influencing drone detection in a binary logistic regression model, which shows that the difference between dew point and temperature significantly influences detection and hypothesize that it is a proxy for other macro weather trends or patterns not measured. Based on our findings, we make recommendations that future nest searching drone research should consider.

ACKNOWLEDGEMENTS

The privilege to participate in this study was made possible by the generosity of Delta Waterfowl Foundation (Delta), and I am grateful to Dr. Frank Rowher for presenting me with the opportunity and Joel Brice for his guidance and inspiration during the whole process. Delta's passion and support for students is demonstrated by the leagues of Delta students that came before me, and their continued efforts to train the next generation of waterfowl biologists. This project would not be possible without the generous financial support from all of Delta's funders and donors, their members who support research projects like this. I would also like to acknowledge the financial assistance from the Safari Club International Manitoba Chapter scholarship.

I want to give recognition to the organizations that have contributed funding and resources to this study, especially the Alberta Conservation Association and the North Carolina Wildlife Resources Commission. In addition, we would like to thank the principal investigators and their graduate students for their collaboration and permission to use their data in this paper: C. Williams and D. Lawson from the University of Delaware; A. Gregory and S. Harsh from South Dakota State University, and T. Hovick and C. Duquette from North Dakota State University.

Thank you to my advisory committee: Dr. Rick Baydack and Dr. Frank Rowher for their advice, support, and patience. I would like to express my sincere gratitude to my primary advisor Dr. David Walker, for their unwavering support and advocacy for me from the beginning. Their mentorship, guidance, and continuous encouragement have undoubtedly provided me with academic and professional opportunities.

I would like to express my heartfelt gratitude to my employer, Manitoba Habitat Heritage Corporation, for their support while completing my thesis. I am grateful for their flexibility and

understanding, which have been immensely helpful in this process.

I would like to extend my sincerest gratitude to my dear friend, Mike Johnson, for their invaluable inspiration, support and guidance throughout this journey. Their willingness to explore concepts and ideas, offer constructive criticism, and serve as a reflecting board has been incredibly beneficial. Their keen insights and thoughtful perspectives have assisted me in navigating the numerous obstacles and challenges I encountered.

Finally, to my loving wife, your unwavering support and encouragement have been instrumental to my success. Thank you for encouraging me to follow my passion and standing alongside me through the ups and downs that came along with it.

TABLE OF CONTENTS

LIST OF TABLES

LIST OF FIGURES

Chapter 1 – Introduction

CONTEXT

The recovery of North American waterfowl populations is undoubtedly one of the 20th century's most significant conservation accomplishments (Mahoney et al. 2015, Nichols et al. 1995). This success is partly the result of intensive science-based research and population monitoring that guides waterfowl management at various scales, such as Habitat Joint Ventures. Nest success is an essential measure in the modelling of population demographics and the development of management plans (Miller and Johnson 1978, PHJV 2021).. Traditional upland nesting surveys conducted in the Prairie Pothole Region typically use the chain-drag method, where researchers drag a cable or chain between two vehicles which flush nesting females from their nests, after which the field crew searches the estimated flush location for the presence of a nest (Higgins et al. 1969, Higgins et al. 1977, Klett et al. 1986). This method requires an investment of personnel, time, logistical planning, and can occasionally cause damage to the nest and adult mortality (Livezey 1980). Recent advances in drone technology have led some researchers to believe we are on the cusp of a technological revolution (Anderson and Gaston 2013, Chabot 2018). It can potentially update his half-century-old method or even supplant it, but only if these approaches can be effective, practical, and improve these surveys. The objective of this Thesis is to assess the efficacy of a commercially available thermal drone system to locate avian nests. The Thesis examines the application of a thermal drone system in multispecies and multihabitat comparisons across North America, and includes a more intensive survey for upland waterfowl. This Thesis provides a proof of concept, evaluates a methodology for field implementation of upland drone nest surveys, and examines factors influencing drone detection.

LITERATURE REVIEW

The literature review focuses on a history and review of nest searching techniques, specifically, the chain drag nest searching method commonly used in the Prairie Pothole Region (PPR). It provides a background review of early drone adoption, its rapid rise and evolution, and an overview of current drone nest searching research. Finally, it provides a brief background of thermography, waterfowl nesting biology, and potential interactions between the two.

Traditional upland nest searching techniques

An intensive nest searching study to evaluate the relationship between waterfowl production and habitat nest site selection was conducted in 1966 by Higgins et al. (1969) in central North Dakota. Before this time, a standardized nest searching technique had not been established to search for upland nesting waterfowl of the PRR. The habitat characteristics of the study area and logistical challenges precluded the researchers from using other documented nest searching methods such as female observation (Earl 1950, Keith 1961) and trained dogs (Bennett 1938, Glover 1956, Keith 1961, Steel et al. 1956). To improve the efficiencies of manual intensive nest searching techniques, the researchers tested a modified cable drag technique drawing inspiration from Lehmann (1941), who used a single 55 – 110 m long 2.5cm inch thick rope or 6.3 mm thick cable dragged behind two vehicles. Higgins et al. (1969) used a shorter (30 m) and thicker (16 mm) cable with chains attached in a series of crescent-shaped loops to aid in the flushing of nesting females. The technique proved effective in detecting nests of upland-nesting waterfowl and upland-nesting shorebirds, especially in areas with dense nesting cover. They also noted flushing ring-necked pheasants (*Phasianus colchicus*) and sharp-tailed grouse (*Tympanuchus phasianellus*).

In 1977, Higgins et al. documented the construction and search method of the cable-chain, after having successfully utilized it for nearly a decade. The technique involves positioning two

vehicles (one of which has a spotter along with the driver) perpendicular to the longest straight edge of the survey plot, with the cable-chain stretched at the appropriate tension. The vehicles traverse parallel to the straight edge. As they reach the edge of the plot, the inside vehicle pivots and realigns to return down its tracks, and the outside vehicle repositions to start the next section of the line transects. Throughout these maneuvers, the spotter constantly observes the cable chain for the presence of a flushing female. Once the researchers observe a flushing female, they stop the vehicles immediately, and the spotter maintains visual contact with the flush location until the driver locates the nest. In 1986 a detailed manual outlining the methodology to study nest success of upland nesting waterfowl in the PPR was published. It introduced using all-terrain vehicles as the tow vehicles for the cable-chain method (Klett et al. 1986).

Researchers adapted Higgins et al. (1969) technique to use a hand-dragged rope with metal cans attached for studies where the cable chain drag is impractical (Duebbert and Kantrud 1974) or for other upland nesting species, such as songbirds that are more fragile (Davis 2003). In addition, nest searching for more cryptic upland nesting species, such as ring-neck pheasant, include radio-telemetry methods where females are captured prior to nesting and outfitted with a radio transmitter to triangulate their nest location after initiation (Dumke and Pils 1979, Whiteside and Guthery 1983).

There is limited research on nest damage by investigators; nest success research methodology suggests removing destroyed nests or expired females (Klett et al. 1986). Other nest dragging studies reported removing investigator-damaged eggs from the nest to reduce predation from olfactory cues (Blythe and Boyce 2020). Investigator egg damage or female mortality is likely common to most nesting studies, but rates are likely low such as the reported 2% (n=7,894) by Higgins et at. (1977).

Drones as an emerging tool

The concept of unmanned aerial vehicles (UAV) has existed for centuries, but their everyday use and early adoption were through military applications (Springer 2013, Custers 2016). The first mention of the word 'drone' was about a UAV in recognition of a British airplane named the Queen Bee that was remotely piloted for anti-aircraft artillery practice in late 1936 (Boyle 2020). Some of the early non-miliary commercial uses of smaller remote piloted drones with habitat management applications included low-altitude rangeland photography using 28 mm – 50 mm film cameras starting after 1989 (Hardin and Jackson 2005, Rango et al. 2006, Quilter and Anderson 2000, Walker 1993). Studies that first documented the use of drones in wildlife applications gained traction in the mid-late 2000s, including the automated detection of birds by Abd-Elrahman (2005) and a proof of concept study showed surveying midsize to large vertebrates with a drone is possible (Jones et al. 2006). Since the 2010s, there has been a rapid rise in drone publications (Chabot 2018). They document drones as a new tool for several survey applications and species groups, praising the precision and efficacy of the tool (Chabot et al. 2012, Chabot and Bird 2013, Koh and Wich 2012, Sarda-Palomera et al. 2012, Watts et al. 2010), and also predict that the technology will revolutionize spatial ecology (Anderson and Gaston 2013).

There have been numerous drone publications (see Chabot 2018 for a summary), but only a few reports on nest detection or searching using a thermal camera, as summarized in Table 1. In these studies, species range in size from small to medium, nesting in various upland and overwater habitats. Quadcopter (4-rotor) drones are the dominant configuration in the studies, with DJI (DJI, Shenzhen, China) being the most common brand. The most common thermal cameras used in these studies are the Tau 640 (FLIR, Wilsonville, OR, USA) or Zenmuse XT (DJI, Shenzhen, China), which uses Forward-looking infrared (FLIR) technology. FLIR cameras detect light in the thermal

portion of the spectrum (wavelengths around 3-12 μm compared to 0.4 to 0.7 μm for visible light). However, most studies have small sample sizes, and only Bushaw et al. (2020*a*) attempted a large-scale comparison to traditional searching methods.

Table 1.1. Summary of thermal drone nest searching studies published 2017 – 2021.

Study	Drone	Thermal camera model, lens, pixel resolution	Species or species groups	Habitat Type	Sample size	Nest detection method	Image processing	Detection Rate
Israel and Reinhard (2017)	8 rotor - Falcon 8 (2.8 kg, 768 x 817 x 160 mm) (Intel, Santa Clara, CA, USA)	Tau 640, 19 mm, 640x512 pixel (FLIR, Wilsonville, OR, USA)	Lapwing (*Vanellus vanellus*)	Agricultural field	15	Automated	Microbolometer optimization algorithm	93 % of known nests
Scholten et al. (2019)	Quadcopter Inspire 1 (3.2 kg 438 x 451 x 301 mm) (DJI, Shenzhen, China)	Zenmuse XT, 9 mm, 640x512 pixel (DJI, Shenzhen, China)	Field sparrow (*Spizella pusilla*)	Grasslands	20	Manual	Real-time visual	85 %
Bushaw et al. (2020*a*)	Quadcopter Matrice 210 (6.4 kg, 716 x 200 x 235 mm) (DJI, Shenzhen, China)	Zenmuse XTR, 19 mm, 640x512 pixel (DJI, Shenzhen, China)	Overwater nesting waterfowl	Prairie pothole wetlands	283	Manual	Real-time visual	34 %

Study	Drone	Thermal camera model, lens, pixel resolution	Species or species groups	Habitat Type	Sample size	Nest detection method	Image processing	Detection Rate
Helvey et al. (2020)	Hex-copter Matrice 600 (9.6 kg, 1668 mm x 1518 mm x 759 mm) (DJI, Shenzhen, China)	Tamarisk 640, 16.7 mm, 640x480 pixel (DRS Technologies, Netanya, Israel)	Mallard (*Anas platyrhynchos*) and blue-winged Teal (*Spatula discors*).	Prairie pothole grasslands	53	Manual post-processing	Min-max normalization, kernel filter, and thresholding	17 % – 38 % based on altitude
Shewring and Vafidis (2021)	8 rotor - Falcon 8 (2.8 kg, 768 x 817 x 160 mm) (Intel, Santa Clara, CA, USA); Quadcopter Inspire 1 (3.2 kg 438 x 451 x 301 mm) (DJI, Shenzhen, China)	Tau 640, 19 mm, 640x512 pixel (FLIR, Wilsonville, OR, USA); Zenmuse XT, 19mm, 640x512 pixel (DJI, Shenzhen, China)	European Nightjar (*Caprimulgus europaeus*)	Clear cut logging sites	2	Manual	Visual post collection inspection	100 %

Study	Drone	Thermal camera model, lens, pixel resolution	Species or species groups	Habitat Type	Sample size	Nest detection method	Image processing	Detection Rate
Stander et al. (2021)	Quadcopter Inspire 1 (3.2 kg 438 x 451 x 301 mm) (DJI, Shenzhen, China)	Zenmuse XT, 19 mm, 640x512 pixel (DJI, Shenzhen, China)	American black duck (*Anas rubripes*), ring-necked pheasant, piping plover (*Charadrius melodus*), passerines	Coastal salt marsh and prairie pothole grasslands	22	Manual	Real-time visual	78 % – 100 % dependent on species site

Thermography review and wildlife applications

Any object above absolute zero emits thermal radiation, known as infrared radiation. Modern commercially available thermal cameras use passive sensors that operate on two spectral bands, middle wavelength infrared (MWIR, 3 – 5 μm) or longwave infrared (LWIR, 8 – 13 μm). Thermal energy directly or indirectly converts into electrical energy. Photon detectors are responsive and effective at detecting a slight temperature difference by directly converting infrared radiation in the MWIR band. However, they are expensive and often require liquid nitrogen cooling to function correctly.

In contrast, LWIR thermal cameras are typically uncooled and use ferroelectric or microbolometer detectors. Microbolometers have higher sensitivity than ferroelectric, have a smaller pixel size, and have the most considerable market share in drone applications (Gade and Moeslund 2014, Havens and Sharp, 2016, Vollmer and Möllmann 2018). Generally, a thermal camera displays a thermal image with a thermal signature (object of interest) which consists of a spectral distribution (wavelength band of infrared energy), spatial resolution (size and shape), and intensity distribution (temperatures). There may also be a temporal component (i.e. moving animal) combined with previous components to make signatures distinguishable from the background (Havens and Sharp, 2016).

Jones (2004) explains that emissivity is a thermal property based on Planck's wavelength distribution function ranging between 0 and 1. Essentially it can be interpreted as a value less than 1 (the value for a perfect emitter known as a blackbody) that measures the ability of the surface to emit thermal energy versus reflect it. For example, a perfect reflector has an emissivity of 0 (low emissivity), whereas a black body has an emissivity value of 1 (high emissivity). Jones (2004) further explains that thermal imagers detect apparent temperatures

which are dependent on emissivity, the Stefan-Boltzmann law, and the temperature of the surface whereby:

$$R \cong \varepsilon\sigma T^4$$

Whereas R = total radiative flux (energy) emitted (and reflected) by the surface substrate, ε = emissivity, σ= Stefan-Boltzman constant, and T = temperature of the surface.

Emissivity is essential because it can affect the apparent temperature of the thermal targets emitted by females and their nests. For example, thermographic research by Best and Fowler (1981) measured waterfowl feather emissivity values and found that the apparent radiant surface temperatures (T_{app}) of Canada geese (*Branta canadensis*) and snow geese (*Chen caerulescens*) relative to ambient temperature (T_{amb}) follow the relationship (in Celsius): $T_{app}= 0.692T_{amb} + 6.103$.

Upland waterfowl nesting biology

Loos and Rohwer (2004) examined nest attendance from 8 species of upland nesting waterfowl in the laying stage (females without a full clutch, traditionally considered in the "laying stage" and not incubating). They found that early laying females increase nest attendance as the laying stage progresses because females tend to leave the nest later each day. Earlier arrival by species, such as blue-winged teal, gadwall (*Anas strepera*), mallard, and northern shoveler (*A. clypeata*), also contributed to increased nest attendance. Their results show that arrival times for laying stage blue-winged teal, gadwall, mallard, and northern shovelers females range between ~0630 hours – 0900 hours, and report departure times for the same species range between ~0700 hours – 2100 hours. In addition, they found that female birds in the initial stages of incubation spend minimal time at the nest, just long enough to lay an egg before leaving shortly after and as laying stage progresses, females arrive earlier and stay later. Based on this study, we presume that females

depart the nest after laying, and do not arrive again until the next day; therefore, nest detection by the drone method during these times may not be possible.

Croston et al. (2020) examined mallard and gadwall incubation recess frequency and timing. The researchers included the day of the year, ambient temperature at the nest, incubation day, and clutch size in their analysis using linear mixed models. Their research findings indicate that incubation recess duration (increased nest attendance) increased as the season progressed, the same trend as laying stage nests in the Loos and Rohwer (2004) study. Croston et al. (2020) report that clutch size and ambient temperature contribute to recess frequency and duration. They reported that female mallard and gadwall are likely to be on a morning recess between 0400 hours – 0700 hours and that recesses may start earlier on warm days and later on cool days. Gloutney et al. (1993) continuously monitored female nest attendance of incubating nests using infrared relays and electronic scales. They report the probability of incubating female presence within 24 hours for all species in our study except northern pintail (*A. acuta*). In addition, their results indicate high nest attendance during overnight hours.

Evaluation of thermal drone detection challenges

Traditional nest searching techniques for upland waterfowl (chain drag or rope drag) typically rely on observing the female attending the nest. These are observer-based methods conducted during daylight hours. Therefore recommendations for timing of nest searches typically consider female nest attendance (dabbling ducks typically take 1 - 2 incubation recesses per day, morning, and afternoon) to maximize female presence and considerations for reducing nest abandonment (Gloutney et al. 1993, Loos and Rohwer 2004, Croston et al. 2020). However, the optimal survey times from these studies range from 0700 hours to 1600 hours and do not consider the possibility

of surveying at night, likely because it is impossible to observe a flushing female or risky to navigate an all-terrain vehicle in the dark safely. Thermal drone nest searching does not have this visual constraint and can operate in the dark. However, thermal drone nesting studies (Bushaw et al. 2020*a*, Stander et al. 2021) report an apparent optimal survey window limited by thermal detection challenges such as false positives, thermal background clutter (see Stander et al. [2021] for a review).

Previous research suggests environmental factors such as humidity can influence thermal camera sensitivity (Havens and Sharp 2016, Stander et al. 2021) or that the emissivity of waterfowl can influence the relative temperatures detected by the thermal camera (Best and Fowler 1981). This results in waterfowl targets that thermally look very similar to their surroundings. Some studies (Bushaw et al. 2020*a*, Scholten et al. 2019, Stander et al. 2021) rely on real-time visual identification for target acquisition. To accomplish this, the drone pilot or thermal video observer relies on the spatial domain (size, shape, intensity, and grouping) of the thermal signals to determine if detected signals should be recorded for ground verification or disregarded as a false positive.

Without the post-processing of thermal images either manually (Helvey et al. 2020) or with the aid of automated algorithms (Israel and Reinhard 2017, Santangelli et al. 2020), detection and recognition by the observer is a necessary step to detect nests using a drone. The observer needs to recognize a thermal signal during the automated flight and judge that the thermal signal is not a false positive. Bushaw et al. (2020*a*) and Stander et al. (2021) have reported challenges with the thermal loading of non-biotic objects (such as rocks and vegetation) increasing as the sun heats the ground and typically starts to occur about an hour after sunrise. Thermal loading continues throughout the day which imposed limitations to using the thermal camera as a survey tool because

the signal intensity from non-biotic caused too much background clutter around this time and throughout the daytime. Background clutter is undesired thermal signals mixed with thermal signals from nests, making it too difficult to identify the target signal from the scene (Havens and Sharp 2016).

Thermal loading is a significant limitation of using a thermal camera because it can cause many false positives (Havens and Sharp, Stander et al. 2021). Therefore, drone flights are conducted at night to maximize nest detection rates due to the high number of competing thermal signals present during daytime flights. However, it can take several hours after sunset for the landscape to reach quasi-thermal equilibrium (when the background, viewed from the thermal camera, is near the same temperature). In addition, thermally loaded rocks are undistinguishable from nests in some cases due to their shape and heat signature (Stander et al. 2021).

PROBLEM STATEMENT AND OBJECTIVES

The use of drones in wildlife research is clearly established (Anderson and Gaston 2013, Chabot 2018, Gonzalez et al. 2016, Hodgson et al. 2016*a*,) and the use of thermal cameras from aerial and terrestrial applications are valuable tools to survey and capture birds (Best et al. 1982, Gillette et al. 2013, Hodgson et al. 2016*a*, Kinzel et al. 2006, Mills et al. 2011, Scholten et al. 2019, Sherwring and Vafdis 2021). Nest searching for avian species with UAS and thermal camera technology is gaining popularity (Bushaw et al. 2020*a*, Helvey et al. 2020, Israel and Reinhard 2017, Santangeli et al. ,2020, Scholten et al. 2019, Shewring and Vafidis 2021). However, there has been little research to examine the application of this technology over a large scale or intensively for upland nesting species. It is also unclear whether the method has equivalent efficacy when compared to ground surveys.

The primary objective of this study is to test the efficacy of a drone with a thermal camera to locate upland waterfowl nests. In addition, we will address the following sub-objectives to achieve the objective:

- Provide a proof of concept for the drone system to search for nests of various upland nesting birds.
- To compare the efficacy of a drone with a thermal camera to the chain-drag method in locating upland waterfowl nests.
- Determine how meteorological conditions influence drone detection.

THESIS LAYOUT

The Thesis is divided into four chapters described below, following the layout of a sandwich-style thesis. Chapters two and three form the body of the thesis, with the former published in the Wildlife Society Bulletin in 2021 and latter with intention to submit for publication.

Chapter 1 – Introduction

This chapter provides the overall context and scope of the thesis. It provides a literature review relevant to the objectives presented.

Chapter 2 – Drone nest searching applications using a thermal camera

This chapter provides the proof of concept for a thermal drone nest searching methodology focusing on upland game and non-gamebird species in North America. It showcases challenges and associated mitigation strategies. The methodology shows potential for adoption as a new nest searching tool.

Chapter 3 – Upland waterfowl nest searching – a comparison between methods and factors

This chapter compares the efficacy of a thermal drone nest searching methodology to the

traditional chain drag method used in prairie waterfowl breeding areas. It also examines factors that influence drone detection nest detection. The results provide considerations for future research.

Chapter 4 – Management implications

This chapter provides an overall summary and provides wildlife professionals with information to consider before implementing the method and widespread adoption.

CONTRIBUTIONS OF AUTHORS

Delta Waterfowl Foundation staff carried out all nest searching. R. Stander led the writing of the thesis, and all other authors listed assisted in revising the published work through constructive comments and editorial support.

Chapter 2 – Drone Nest Searching Applications Using a Thermal Camera

FOREWARD

In an age of rapidly evolving drone technology, we embark on a large-scale drone nest searching testing mission to provide broadly appliable advice to other wildlife professionals. We flew and drove across North America in a single nesting season to survey birds during optimal nesting periods collaborating with researchers from four other institutions and organizations. The chapter explicitly addresses Objective 1 of the Thesis. This chapter tests the thermal drone nest searching method in various habitat types for several upland nesting species spanning a large geographic area. It uses a single fixed survey methodology to assess the efficacy under different conditions. It highlights the potential challenges and mitigation strategies. This chapter was published as Stander, R., D. J. Walker, F. C. Rohwer, and R. K. Baydack. 2021. Drone nest searching applications using a thermal camera. Wildlife Society Bulletin 45: 371-382. doi.org/10.1002/wsb.1211 under Emerging Issues in the Wildlife Society Bulletin on 13 September 2021.

INTRODUCTION

Cable chain-drag (Higgins et al. 1969, Klett et al. 1986), rope drag (Labisky 1957), female observation (Martin and Geupel 1993), and territorial pair behavior (Murphy et al. 1999) are all standard nest searching methods for many avian species. However, traditional methods are labor, time, and cost intensive (Desante and Geupel 1987, Ralph et al. 1993), can reduce nest success (Livezey 1980, Götmark 1992) and cause nest abandonment during ground visits (Evans and Wolfe 1967, Lloyd and Plagányi 2002).

The use of unmanned aerial systems (UAS), hereafter drones, in wildlife research is well documented (Anderson and Gaston 2013, Gonzalez et al. 2016, Hodgson et al. 2016*a*) and thermal cameras from aerial and terrestrial applications have been shown to be useful tools to survey and capture birds (Best et al. 1982, Kinzel et al. 2006, Mills et al. 2011, Gillette et al. 2013, Hodgson et al. 2016*a*). Species such as ring-necked pheasant (*Phasianus colchicus*), which have high nest abandonment rates (Evans and Wolfe 1967), may be more effectively surveyed using aerial drone systems. Disturbance by drones is species and platform specific (Mulero-Pázmány et al. 2017) and can be mitigated by adopting best practices as outlined by Hodgson and Koh (2016).

Nest searching for avian species with the aid of a thermal camera has been explored to varying degrees of success (Israel and Reinhard 2017). In a study by Boonstra et al. (1995), researchers were able to clearly record thermal signatures from known ground and cavity nests for a variety waterfowl and woodpecker species but were unable to find new nests. Galligan et al. (2003) found that thermal cameras aided traditional searching and census methods by increasing efficiency of finding cryptically camouflaged nests, while resulting in less disturbance to both the nest and surrounding vegetation. Nest searching, as with many thermal imaging studies to date, incorporates primarily manual (visual) target identification by the researcher (for a review see McCafferty 2013, Havens and Sharp 2016); however, several automated approaches to animal identification are currently being developed. Automated thermal target detection using drones has been successfully demonstrated with several species of large mammals such as American bison (*Bison bison*, Chrétien et al. 2015), cattle (Longmore et al. 2017), elk (*Cervus canadensis*, Chrétien et al. 2015), fallow deer (Dama dama, Chrétien et al. 2015), grey seal (*Halichoerus grypus*, Seymour et al. 2017); grey wolf (*Canis lupus*, Chrétien et al. 2015), hippopotamus (*Hippopotamus amphibius*, Lhoest et al. 2015), and white-tailed deer (*Odocoileus virginianus*, Chrétien et al.

2016). Automation has been primarily applied to large animal species with few studies focusing on smaller target species, although low altitude thermal imaging has been automated for rabbit and chicken detection (Christiansen et al. 2014).

To date there have been no studies evaluate thermal drone technology using a consistent, fixed-survey methodology, applied across multiple habitats over a large geographic region to locate avian nests. The main objective of our study was to assess the efficacy of a commercially-available, thermal drone system to locate nests using multiple case studies of game (Anseriformes and Galliformes) and nongame bird species (Passeriformes and Charadriiformes) occurring in a variety of habitats within North America. We also identified several challenges that need to be addressed prior to the practical application of this technology by wildlife managers.

STUDY AREA

We conducted nesting surveys across 7 different ecoregions in the US and Canada and in several natural and planted habitat types (Fig. 2.1; Table 2.1). Each site focused on one species or group of species (e.g., Anseriformes and Passeriformes) and sites ranged in size from 8.1 ha to 16 ha. Anseriformes sites were in the continental US. American black duck (*Anas rubripes*) study sites were uplands surrounding brackish salt marshes in North Carolina. Other upland nesting waterfowl sites were in dense cover in the Prairie Pothole Region of North Dakota. For Galliformes, ring-necked pheasant sites were in lowland cattail and prairie grasses complexes in South Dakota, and the Hungarian partridge (*Perdix perdix*) site was located in mixed grasslands in Alberta, Canada. Passerines sites were in the grasslands of the Missouri Coteau in North Dakota, and piping plover (*Charadrius melodus*) study sites were located near gravel shores of alkali lakes in Alberta.

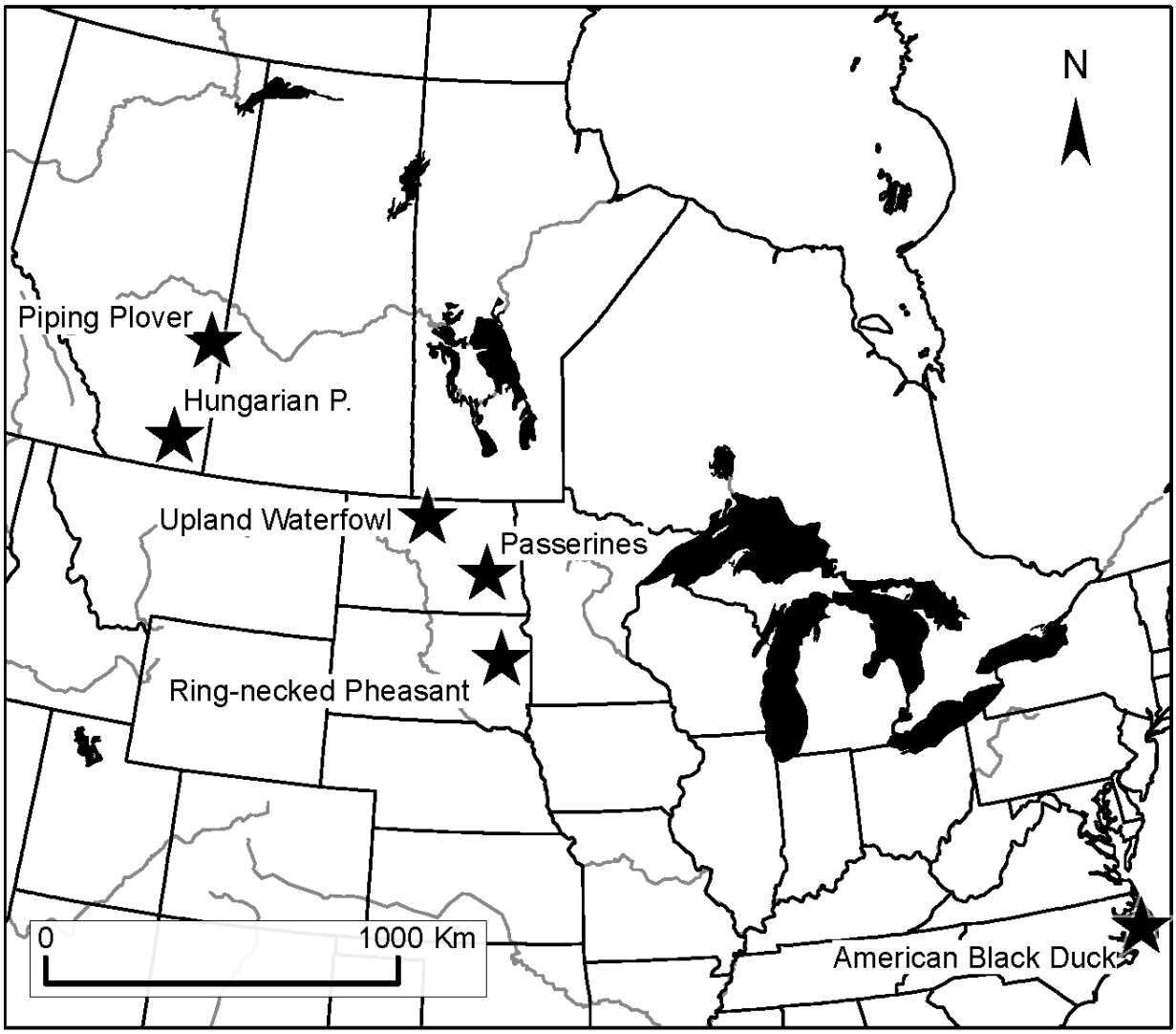

Figure 2.1. The 7 study locations (stars) in North America. Three sites were in western Canada and the remaining sites were in the United States.

Table 2.1. Site information for the species or groups included in the 2017 study area within North America (see Fig. 2.1 for corresponding map).

Species or Groups	Location	Latitude, Longitude	Ecoregion and Habitat	Site sizes (ha)	Number of sites
American black duck (*Anas rubripes*)	Pamlico sound, NC	35.346874, -76.346409	Chesapeake-Pamlico lowlands and tidal marshes. Brackish tidal marsh.	4–12	4
Upland waterfowl	Cando, ND	48.355231, -99.338229	Glacial Lake Basin. Conservation Reserve Program (CRP) dense nesting cover.	4	2
Ring-necked pheasant (*Phasianus colchicus*)	Virgil, SD	44.310759, -98.411460	James River Lowland. Cattail stands and prairie grasses.	10	1
Hungarian partridge (*Perdix perdix*)	Lethbridge, AB	50.192294, -112.463265	Mixed Grassland. Planted forbs and shrubs part of an upland restoration and enhancement project.	8	1
Piping plover (*Charadrius melodus*)	Provost, AB	52.539621, -110.009912	Dry Mixed Grassland. Gravel shorelines of alkali lakes.	1–4	6
Passerines	Streeter, ND	46.722773, -99.445926	Missouri Coteau. Native cool season grasses, with invasive grasses and forbs in rotational pastures.	4	1

METHODS

Data Collection System

The drone deployment setup and configuration (Fig. 2.2A; Table 2.2) consisted of a commercially available quadcopter drone (Inspire 1 v. 2.0) with a Zenmuse XT 19mm thermal camera and a Zenmuse X3 35mm equivalent camera . And 9 TB48 batteries (drone, cameras, and batteries from DJI, Shenzhen, Guangdong, China), which were charged on a Smart Power Charge M100 (Intellitrax Inc, Newton, AL, USA) 4-bank rapid charger powered by a Generac ix800W (Generac Power Systems, Waukesha, WI, USA) inverter. We used 2 iPad Mini 4s (Apple Inc, Cupertino, CA, USA) for redundancy in case of iPad failure and for increased flying time (the iPad could not

be charged while operating the drone and needed to be swapped out for sustained operation). Using the above hardware configuration, we were able to continuously operate the drone as the batteries were cycled through the charging equipment. We followed 14 CFR Part 107 Small Unmanned Aircraft Systems to obtain a commercial pilot license for drone operation in the US. Transport Canada accepted the US credentials allowing the pilot to fly the drone at study sites in Canada. To operate at night in the US we obtained a 14 CFR § 107.29 Daylight operation waiver # 107W-2017-00986 from the FAA, and in Canada we obtained a Special Flight Operations Certificate RMDIS # 12889587 from Transport Canada. As per night operation requirements we outfitted the drone with a DS-30 white strobe light (North American Survival Systems, Poulsbo, WA, USA). We used SkyVector (SkyVector 2021)) to ensure that restricted airspace was avoided. As required by our permits, we used a visual observer (for night in the US and day and night in Canada) to maintain a visual line-of-sight of the drone during flight operation.

Table 2.2. Drone and thermal camera specifications for the system used in this study. Most descriptors are self-evident, except for noise−equivalent temperature difference (NEDT), field of view (FOV) which includes angles with respect to height and width of the image, and instantaneous field of view (iFOV) in milliradians.

Equipment	Specifications
Inspire 1 Drone	
UAV type	Quadcopter drone
Model	T600
Weight (without thermal camera)	3060 g
Max. flight time	± 18 minutes
GPS hovering accuracy	Vertical: ± 0.5 m Horizontal: ± 2.5 m
Battery	5700 mAh 6 cell lithium polymer (TB48)
Zenmuse XT Camera	
Thermal imager type	Uncooled VOx Microbolometer
Pixel pitch	17 μm
Spectral band wavelength	7.5 μm – 13.5 μm
Focal length	19 mm
Aperture (fixed ISO and shutter)	*f*/1.25
Sensitivity (NEDT)	<50 mK at f/1.0
Field of view (FOV)	32°w x 26°h
Instantaneous field of view (iFOV)	0.895 mrad
Image size	640 pixels x 512 pixels (0.32 Megapixels)
Sensor dimensions	10.88 mm x 8.84 mm
Ground sampling distance (GSD)	4.1 cm/pixel
Radiometric resolution	8 bit or 14 bit raw
Camera dimensions	103 mm x 74 mm x 102 mm
Weight	270 g
Footprint at nadir[a]	26 m x 21 m (width x height)

[a]Flown at an altitude of 46 m agl.

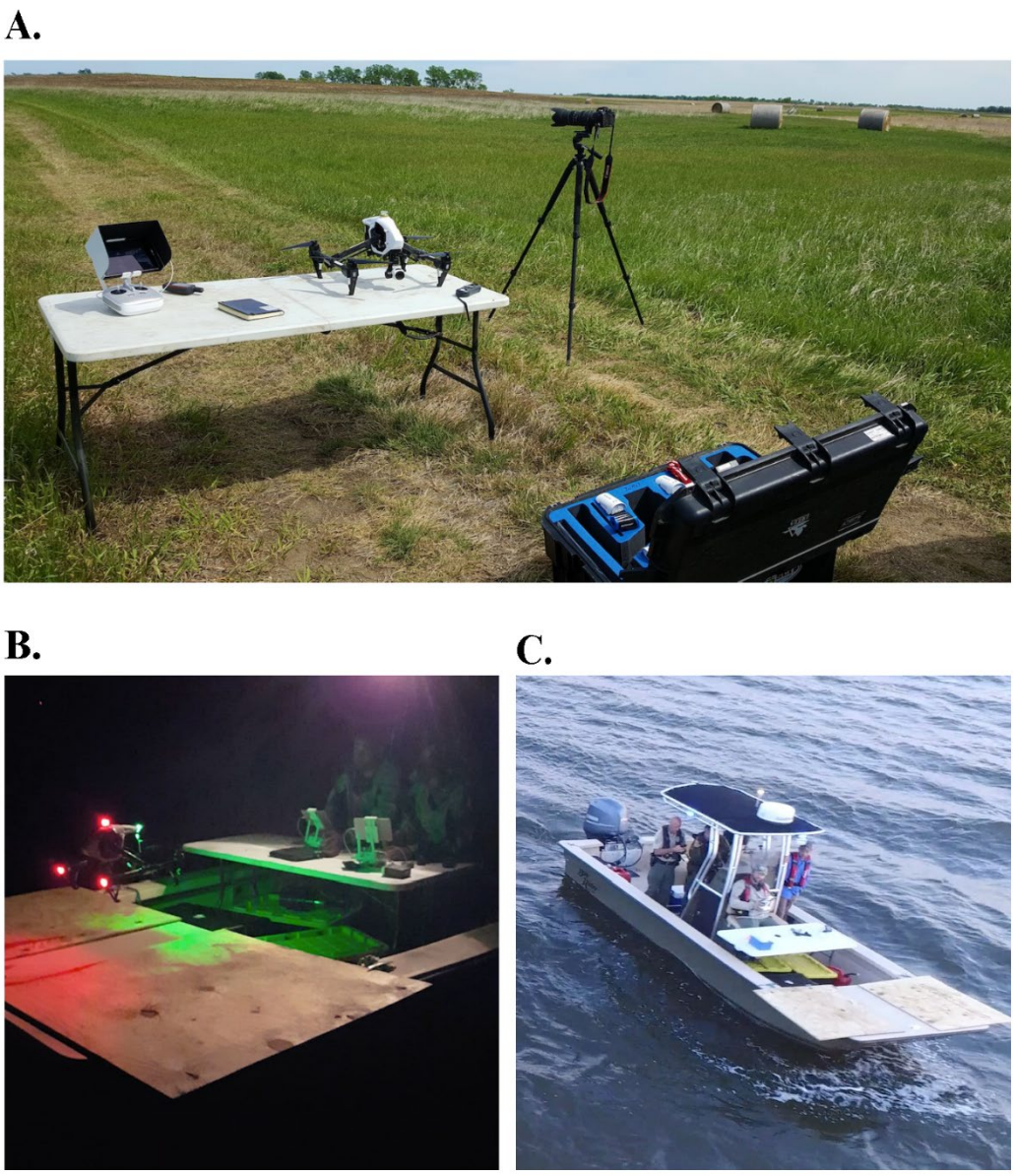

Figure 2.2. Ground control station set-up at the point of drone deployment: A) example of a typical set-up in South Dakota for the ring-necked pheasant nest survey 16 May 2017; B) modified deployment in the North Carolina American black duck salt marsh site with night flight take-off and C) early morning landing approach. Plywood was used to provide a larger landing surface, but the drone can be easily launched from a 1.5 m x 1.5 m platform.

Software

iOS software programs included DJI GO and DJI Ground Station Pro (DJI, Shenzhen, Guangdong, China) and Tag Pilot (Drones Made Easy, San Diego, CA, USA). We used Tag Pilot for target identification and for recording GPS locations. During sampling, all recorded locations are displayed real-time on the iPad, and the coordinates stored as decimal degrees in KML format using the WGS 84 (EPSG: 4326 projection). We exported coordinates to a handheld Garmin 64 S (Garmin LTD, Schaffhausen, Canton of Schaffhausen, Switzerland) for ground verification.

Nest Searching Methods

We conducted drone nest searching surveys during the breeding season from 15 May–17 June 2017, during nighttime hours (2300 hours–0700 hours CST) to maximize temperature contrast between nest targets and background by allowing the environment to reach thermal equilibrium (Boonstra et al. 1995, Galligan et al. 2003, Havens and Sharp 2016). We used an aerial point transect survey (Strindberg et al. 2004) and combined all points into an aggregate sampled transect.

The point transect method consisted of a series of rotational points systematically distributed throughout the survey site (either along a transect or in a grid pattern). Point spacing ranged from 30.5 to 121 m and depended on flight altitude above ground level (agl), which influences the size of the sensor footprint. At each spacing distance we ensured that there was overlap between viewing angles at each point locations. For example, at 46 m agl, the sensor footprint is 26 m x 21 m at nadir (camera point directly at the ground below the drone), which provides a ground sampling distance of 4.1 cm/pixel and there was an overlap of 3 m between each viewing angle and survey points. An illustration of a point sample taken by the drone and associated footprint sizes for the 3 gimbal look-angles used in the survey per point is shown in Figure 2.3. At each sample point the camera was rotated once at nadir (gimbal angle = 0°, cone

denoted by the solid line in the upper figure and then twice more after adjusting the gimbal angle by 20° (Φ_1, denoted by dashed cone) and 40° (Φ_2, denoted by dashed-dot cone). The oblique gimbal

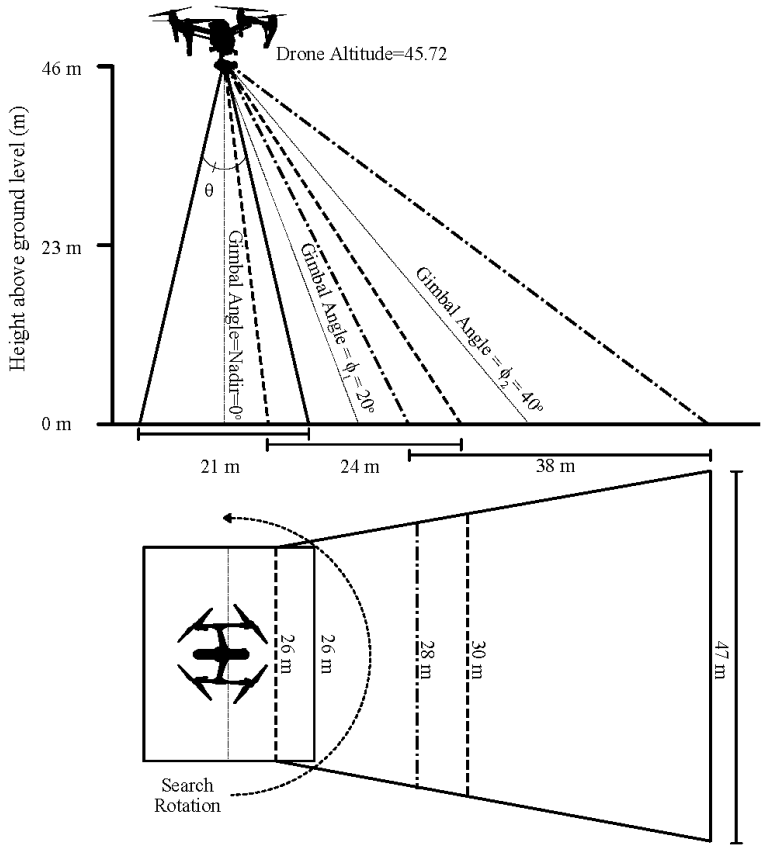

Figure 2.3. Point transect sample spacing, thermal drone sensor footprint, and drone rotation illustration.

look-angles result in non-square footprints (isosceles trapezoids, in the lower portion of the figure), the height of the footprints is provided by the horizontal rulers and widths by the vertical ruler or lines (line styles of solid, dashed and dashed-dot correspond to the look-angles described above). This results in larger footprint size as gimbal angle increases (for example, the footprint at nadir was 546 m^2, and at a gimbal angle of 40° it was 1425 m^2). In this example, all footprint calculations are based on equations in Havens and Sharp (2016) using the camera specifications from Table

2.2, and a height of 46 m agl using the camera's vertical field of view (VFOV = θ) of 26°. All values are rounded to the nearest meter or degree. The thermal signature of most species in the study (except for Passeriformes) were expected to be more than 12 pixels at an agl of 46 m.

We made additional considerations for increased vegetation cover as nesting season progressed, desired site coverage, and respective species size. For example, we spaced upland waterfowl points 121 m apart at an agl 46 m (as described above) and spaced passerine point samples 30.5 m apart at an agl of 23 m (ground sampling distance of 2 cm/pixel and four times the resolution). Modifications were also made at piping plover nest sites to account for the presence of predator exclosure cages (Schemlzeisen et al., 2004). At the piping plover study site search methodology focused on collecting detailed imagery at altitudes from 30 m to 15 m above the known nests while performing the search transect adjacent to the cages to look for other nests.

At each survey point, nest searching commenced in a series of systematic circular rotations starting with the camera pointing directly towards the ground. We then rotated the drone 360° around the sample point at an optical axis of ~ 20° from nadir (Fig. 2.3). Following the first scan we adjusted the optical axis of the camera to ~ 40° from nadir (increasing the viewing angle more obliquely) and performed a new search. We estimated the optical axis based on overlap of the frames between viewing angles and a reference target within that overlapping area. An identifiable object or feature near the top of the field of view (FOV) for the current viewing angle (typically within 2 m from the edge at 46 m agl) would be placed at the bottom of the FOV for the next viewing angle in the matching location. We conducted 3 rotations (i.e., 3 viewing angles) per point (Fig. 2.3), covering ~ 1.2 ha (at 46 m agl). At a typical flight agl of 46 m it takes 2.5–3.75 minutes to cover 1,000 m^2. Our drone configuration allowed for 20 minutes per flight, and multiple flights were required to completely survey a transect. The drone was programmed to return to the previous

last position following a battery swap.

We paused the searching when we identified an unidentified target of interest and hovered the drone directly above the target for nest determination. We observed the target for a short period (<10 seconds) to determine if the thermal signal was a potential nest. For example, some targets were mobile; we readily identified flying passerines by their fast-wing beats, and large-target movements were associated with small mammals. If the target was stationary, we examined it to determine if the outline of a nest bowl, attending bird, or exposed eggs were visible, but even if not, all thermal target locations were collected. Images of an American black duck female on a nest at three altitudes highlight the typical search image (Fig. 2.4). We recorded GPS coordinates of targets using Tag Pilot when the drone hovered directly over the target, with the center of the camera FOV orientated at nadir. After the coordinates were recorded using Tag Pilot, searching resumed from where it paused using Ground Station Pro for spatial reference. Our approach took multiple flights to survey one site, sampling took an average of 2.5–3.75 minutes to cover 1,000 m^2.

We flew multiple consecutive nights when possible to increase sample effort and to reduce false-positive thermal targets. We surveyed 4 nights for ring-necked pheasants, 3 nights for Hungarian partridge and grassland passerines, and 2 nights for upland nesting waterfowl. Repeated surveys were planned for coastal marshes, but these could not be completed because of weather and logistical challenges. We determined nest presence or absence by ground verification immediately following the final night of flights for upland waterfowl, American black duck, and passerines. In addition to determining presence or absence of a nest in upland waterfowl sites,

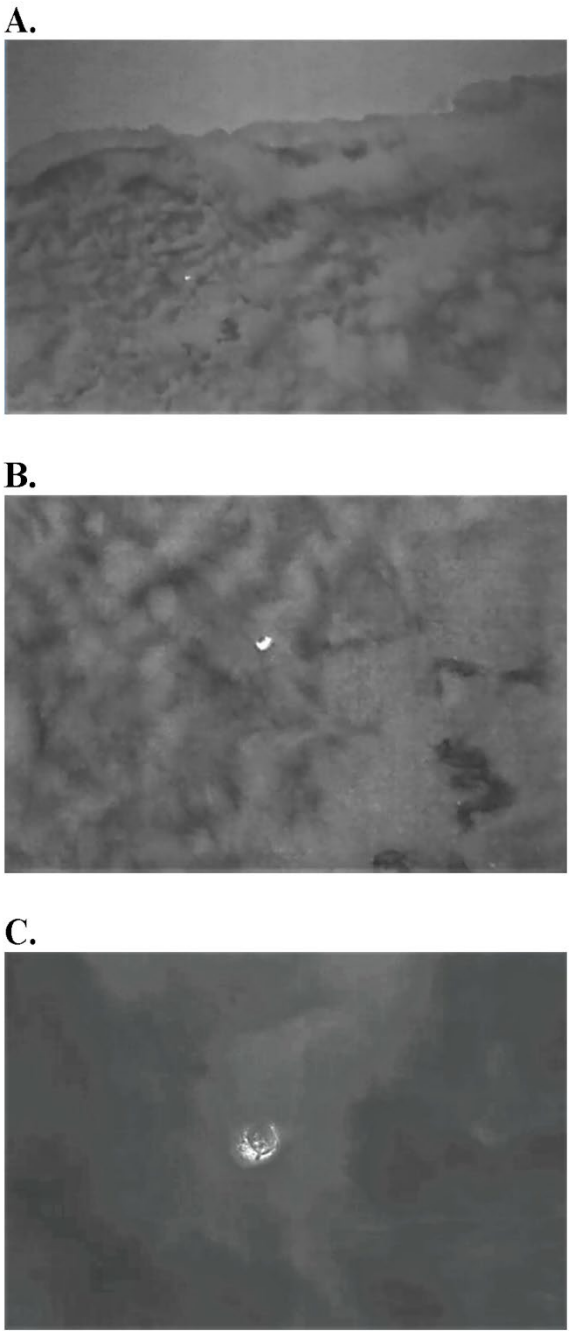

Figure 2.4. Thermal images of a nesting American black duck taken in Pamlico sound. Image A) at the survey standard altitude of 46 m agl appearing as a single point; B) at 20 m agl with a crescent shape; and C) at 10 m agl where the female duck can be seen in silhouette.

we measured nest incubation stage by candling the eggs following methods by Weller (1956). For upland waterfowl and passerines, we inspected all identified locations for nests, but for American black ducks we only inspected locations that were not identified as a clapper rail (*Rallus crepitans*) at a nest. Clapper rails were evident by a long bill visible in the thermal imagery during the drone survey (we verified a subsample [n = 5] of suspected clapper rail nests for the presence of a nest, which were confirmed). For ring-necked pheasants, consecutive surveys occurred for 4 nights. We conducted ground verification at locations where ≥3 points from consecutive nights overlapped by ≤3m. At the ring-neck pheasant study site nest abandonment was a concern and therefore we did not perform ground verification until the radio-marked female stopped displaying nesting behavior. We used ArcGIS (ESRI, Redlands, CA, USA) to analyze overlap between drone determined nest locations and field determined locations. We considered a nest present (matched between drone and ground sampling) when the Tag Pilot location was ≤10 m from the field nest coordinates.

To compare drone nest searching to traditional methods we relied on independent nest searching studies done by partner groups and agencies. In conjunction with ongoing research, Delta Waterfowl Foundation searched upland waterfowl sites using traditional chain-drag methods (Higgins et al. 1969, Klett et al. 1986) 4 to 7 days prior to the last day of drone flights, North Dakota State University searched grassland passerine sites 2 weeks prior for all grassland nesting species following methods outlined by Hovick et al. (2012), University of Delaware searched American black duck sites using a modified rope drag method (Lawson et al. 2017) 7 days prior to the drone flights, Alberta Conservation Association searched piping plover sites during an annual census following methods by Goosen (1990) 1 to 2 days prior to drone flights, South Dakota State University located the ring-necked pheasant nest using telemetry following methods outlined by

Stackhouse (2013). No traditional nest searching occurred prior to the drone flights at the Hungarian partridge site and therefore no known nests were present. In this study we define a false positive as any thermal target that did not match a target species nest, or that could not be located or otherwise verified by ground-based survey. In the results we report nests as found only if they were ground verified as a target-species nest.

RESULTS

Anseriformes

The sites sampled for American black ducks had 2 nests that were active during our aerial surveys; although not the focal species of the survey site, clapper rail nests were also found. We identified 40 targets at both American black duck and upland nesting waterfowl sites. Thermal targets were verified to include the 2 known nests and an additional 14 clapper rail nests; the remaining 24 targets were false positives (Table 2.3). We were unable to perform repeated surveys as planned for the American black duck study site because of potential risk to the equipment or operators inherent to operating in a marine environment, and the nest density. The American black duck nests we found were in dense surrounding vegetation (primarily *Spartina patens, Distichlis spicata*, and *Juncus roemerianus*). At the American black duck study site the transect sampling occurred along the first 46 m of shoreline (i.e., flight path followed the shoreline) where higher nest densities are expected (Lawson et al. 2017). We modified the control station for the drone pilot to take off from a platform on a mobile boat to stay within operational range of the drone (Fig. 2.2B, 2.2C).

The upland waterfowl sites sampled in North Dakota had a total of 18 known nests located using chain-drag method. There were 62 thermal targets identified using the drone of which 39 were false positives. The remaining 23 thermal targets were ground verified as 18 nests (14 known

nests and four additional nests located only using the drone method). Five of the 18 nests were observed on both survey nights (Table 2.3). Two of the 4 additional nests were in incubation during the chain-drag survey, which included a northern shoveler (*Spatula clypeata*) nest at 14-days incubation and a lesser scaup (*Aythya affinis*) nest at 8-days incubation (therefore at 7- and one-day incubation respectively at the time of the chain-drag survey). The other 2 nests were at laying stages of incubation during the chain-drag survey, but all were within the survey area. During the drone survey we observed the formation of radiation fog (ground or valley fog) in low lying areas.

Galliformes

The drone survey area had one active, radio-marked nesting female ring-necked pheasant. We identified a total of 151 targets over the 4 survey nights, of which 143 were false positives. The remaining 6 thermal targets were ground verified as 2 nests (the known and one additional nest) that were observed 3 of the 4 survey nights (Table 2.3). Because of high nest abandonment, the two nests were verified later in the breeding season, after the known nest hatched. The additional nest was confirmed by the evidence of a nest bowl, egg fragments and membranes at the GPS location. We observed ring-necked pheasants in a variety of cover from thick cattail (*Typha* spp.) stands to medium and short types of mixed prairie grasses; this species' thermal signals were characteristic of their body shape and plumage. An image captured at a reduced flight altitude shows the species identifying characteristics in high detail (Fig. 2.5A); however, body shape and plumage were also observed at survey altitude. We observed dry residual vegetation and weather conditions at the site leading up to the sampling period. One thunderstorm occurred between sampling nights.

We identified a total of 40 targets over the 3 survey nights at the Hungarian partridge site in southern Alberta. Five thermal targets were observed on 2 nights within proximity of each other,

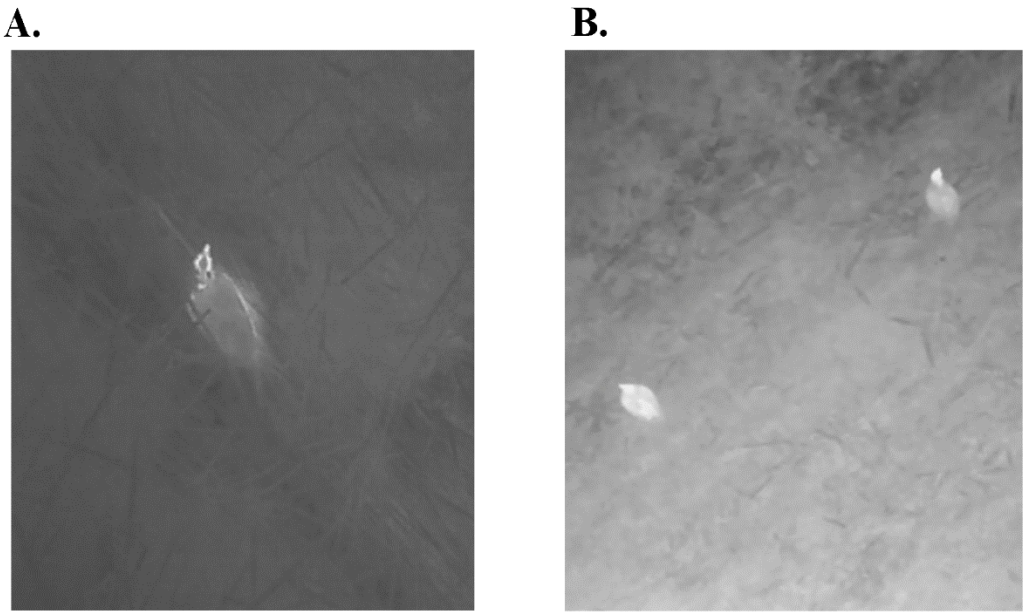

Figure 2.3 Thermal images of A) Ring-necked pheasant in Virgil, SD, and B) Hungarian partridge in Lethbridge, AB Canada. Both species were easily identified in thermal images while roosting.

but no nests were found (Table 2.3). We clearly observed adult birds in thermal imagery (Fig. 2.5B) and based on inspection of the thermal targets during drone sampling, we observed a suspected nest with visible eggs. Ground verification occurred 25 days after drone surveys; after the nesting period but no residual nest materials were found. Rain during sampling reduced search time to less than 15 minute windows on most nights and on the only clear night there was a high humidity level.

Table 2.3. Breakdown of nest detection details for thermal targets identified using the drone method.

Species or species group	Known target species nests[a]	Thermal targets	Known target species detection rate	Additional nests identified by drone	Nests identified ≥ one night[b]	False positives
Anseriformes						
American black duck	2	40	2 (100%)	0 (14[c])	n/a	24 (60%)
Upland Waterfowl	18	62	14 (78%)	4 (0)	5	39 (63%)
Galliformes						
Ring-necked pheasant	1	151	1 (100%)	1 (0)	6	143 (95%)
Hungarian partridge	0	40	n/a	0 (0)	0	40 (100%)
Passerines	1(1[d])	28	1 (100%)	0 (2[d,e])	0	25 (89%)

[a]Non-target species nests that were known or discovered using the drone shown in parenthesis. [b]May include multiple records of a single nest found multiple nights. [c]clapper Rail. [d]mallard. [e]pintail.

Other species

Piping plover surveys in Alberta focused on 3, 0.8 ha shoreline sites, each containing one known nest protected by a predator exclusion cage. At all 3 sites, we detected heat signatures from females attending the nests flying the drone at altitudes ranging of 20–30 m agl on all repeated nights. The cage itself appeared cool in the thermal image but did not obstruct the nest thermal signature at the tested altitudes (Fig. 2.6A). We also conducted a transect survey, in which we discovered a savannah sparrow (*Passerculus sandwichensis*) nest.

The grassland passerines site in North Dakota had a grasshopper sparrow (*Ammodramus savannarum*) nest and a mallard (*Anas platyrhynchos*) nest. We identified a total of 28 targets during the 3 nights, of which 25 were false positives. The remaining 3 thermal targets were ground verified as nests (both known nests and one additional northern pintail [*A. acuta*] nest). No nests

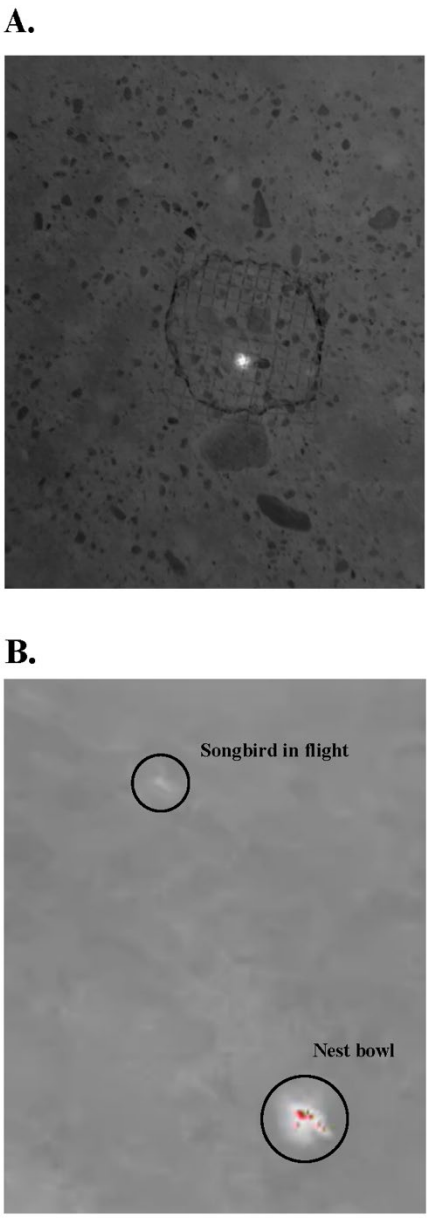

Figure 2.4. Nongame bird nest-searching included A) piping plover in Provost, Alberta, Canada, where the nest and nest-cage installed to protect the site can be clearly seen (the cage is cooler than the surrounding nest and ground), and B) a passerine in Streeter, North Dakota, where the nest bowl, eggs and residual thermal signature of the adult bird can be seen (adult was in flight at time of image capture).

were detected on multiple nights (Table 2.3). Some of the false positives were suspected as nests; we observed songbirds moving on and off structures that appear as nest bowls containing egg-like objects in the thermal imagery (Fig. 2.6B). We were unable to locate suspected nests during ground verification surveys. Heavy rain and high winds were observed during the sampling effort.

Challenges

At each survey site it was evident that the signal quality and detectability of the thermal drone method was being influenced by microclimate and habitat effects. The challenges and possible mitigation strategies are summarized in Table 2.4. We found the thermal signal attenuating or interfering effects not to be species specific and were common at many sites. Here we illustrate the best examples of these challenges. At the American black duck site, we noticed the habitat to exhibit thermal signal shielding properties. For example, we placed a thermal target (near 36º C) under typical dense nesting cover (*Spartina patens*), altitudes higher than 10 m the target was no longer visible to the sensor (Fig. 2.7A).

False positives from generated from non-nest objects were also a challenge. For example, under warm conditions, daytime thermal loading of objects such as rocks occurs and was particularly problematic (Fig. 2.7B). False positives from identified sources included roosting birds (such as the ring-necked pheasant site); nocturnal mammals; soil mounds created by ants and fossorial species; surface substrate and features (such as rocks (Fig. 2.7B) at the passerine site); water features (such as cattle tracks (Fig. 2.7C) observed at the piping plover site); burrows or holes; fence posts; tree stumps; bovine feces. Additionally, lunar illumination or reflection (Fig. 2.7D) was clearly visible at sites near water but effects on detectability was not quantified.

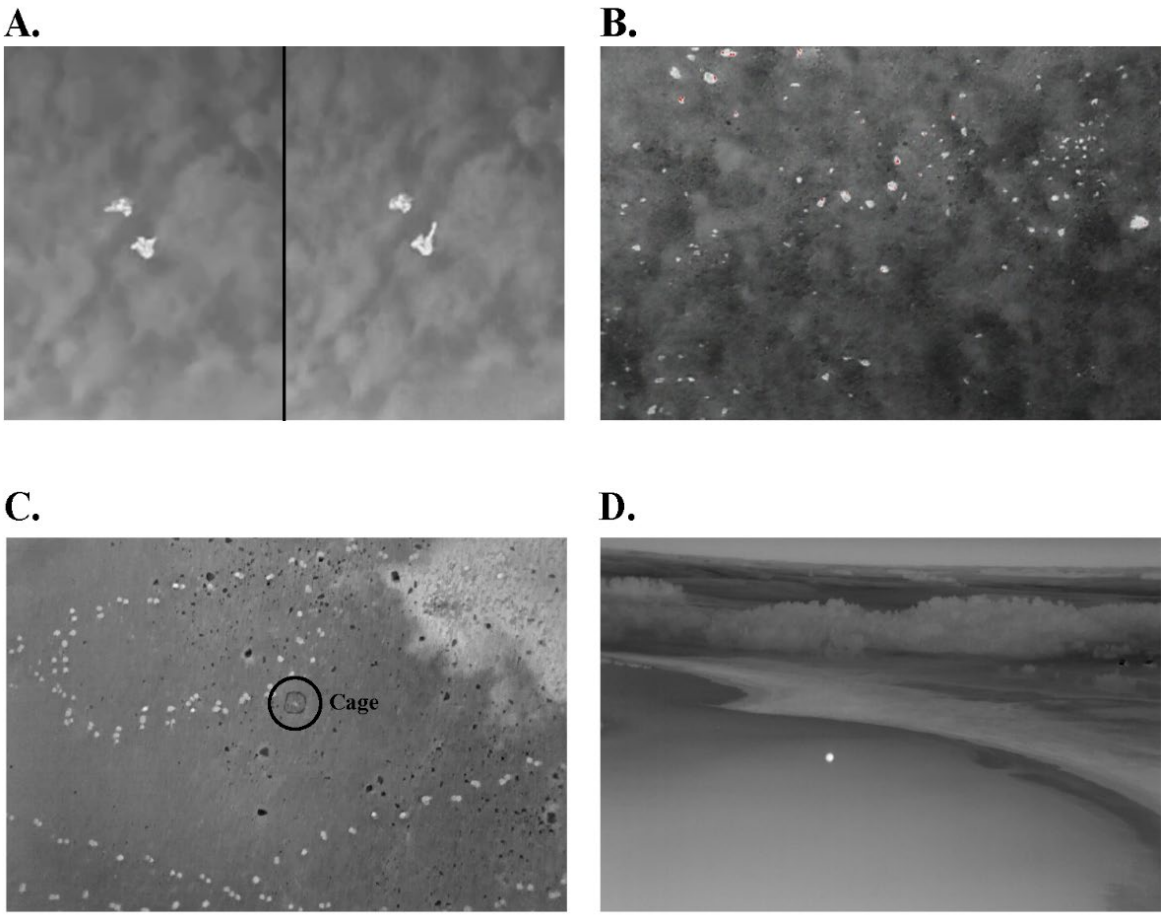

Figure 2.5. Examples of confounding thermal signatures and challenges in application of thermal drone surveys: A) thick cover of vegetation demonstrated by author extending arm under a clump of *Spartina patens* (Fig. 2.7A left frame) and then removing it (Fig. 2.7A right frame), B) rocks with a thermal loading well above the background, C) thermal image of a shoreline, dark spots are rocks and bright spots are cattle tracks with water in them, the predator exclusion cage can be seen slightly above center frame as a dark ring with the thermal signature of the bird in the middle, and D) lunar reflectance from a wetland with a pasture and fields behind (dark exposed soil and warmer vegetation and tree-line).

Table 2.4. Nest searching summary of species including microclimate and habitat, and macro influences on thermal imagery, types and magnitude of errors and possible mitigation.

Groups/Species	Microclimate and Habitat Effects	Macro influences	False positives and nest detection	Suggested Mitigation
American black duck	Thermal shielding from dense nesting cover.	High humidity decreased detectability.	Large number of targets seen but not identified. All known nests found.	Use nadir look-angle. Cover larger area faster and search for easily identifiable nests. Lower altitude investigation of targets.
Upland nesting waterfowl	Some thermal shielding from vegetation. Rocks, anthills, and waterbodies caused false positives.	Ground fog in low lying areas, esp. predawn.	High number of false positive. Not all nests detected. Variable detection with revisits. Found nests missed by chain drag.	Optimal conditions observed during slight to moderate breeze during cloudy day. Sample to avoid water. DGPS or alternate software for increased position accuracy. Lower altitude investigation of targets.
Ring-necked pheasant	High visibility for species (potential morphological difference) in residual dry vegetation.	Early dry conditions seem to enhance detectability.	Numerous false positives detected. Variable detection with revisiting. All known nests located.	Lower altitude investigation of targets. Technique may also be useful for population surveys or capturing birds.
Hungarian partridge	Habitat restoration site with relatively low vegetation, but exposed rocks.	Thermal scattering from meteorological conditions. Large day and night temperature differences causes false positives from rocks.	Numerous false positives. One nest visualized but not verified. Poor weather hampered species study.	Investigate impact of lunar reflectance on constant thermal target. Sample close to background thermal equilibrium near and after dawn.
Grassland passerines	Thermal signatures from solar loaded rocks.	Large day and night temperature differences, and rain.	Large number of false positives. All known nests located.	Sample close to background thermal equilibrium near and after dawn. DGPS or alternate software for position accuracy.
Piping plover	Thermal signatures from water in cattle tracks. In absence of vegetation rocks appear cool.	Large day and night temperature differences.	All known nests detected, cages being highly visible. False positives from water in cattle tracks and other depressions.	Sample close to background thermal equilibrium near and after dawn.

DISCUSSION

Our study demonstrates that nests for a wide range of avifauna, occurring in a variety of habitats, can be detected using thermal imaging from commercially available drone systems. No study to date has attempted to apply thermal imaging using current drone technology across such a diverse range of species targets and conditions. Maximizing sample size for a study at multiple sites within

the same nesting season is challenging; however, there is value in applying a consistent and standardized methodology over multiple species, sites, and habitats to allow comparisons of the efficacy of this new nest searching tool. Although sample sizes are too small to statistically compare detection rates, we detail several observations here that will assist biologists in planning future thermal imaging studies.

First, aerial thermal surveys are often associated with a high number of false positives (Johnson and Ross 2008). At some of our study sites 100% of detected thermal signatures were determined to be false positives. In thermal imagery, a wide range of sources produce thermal signals (Havens and Sharp 2016) which can be indistinguishable from nests. We categorize near-ground inanimate sources of false positives and conditions that cause thermal signal attenuation as microclimate and habitat sources. We experienced challenges with image contrast during high humidity especially prior to sunrise, creating changing microclimate conditions within a single night's survey and across different sample nights. High humidity was observed in low-lying areas and within vegetation cover but was not directly measured. This occurred in both coastal and upland areas and was influenced by topography. Coastal areas or topographically complex landscape with low-lying areas inherently have higher humidity rates associated with them, which may become trapped in the dense grass causing an absorption of infrared energy

We categorize sources of false positives and signal attenuation not specific to near- ground conditions as macro influences. These include weather patterns and associated atmospheric conditions, and astronomical conditions. Weather conditions (e.g., rain, winds) can often interfere with sampling and under extreme conditions sampling may need to be forfeited. At sites, such as the Hungarian partridge site, where high humidity levels persisted after rain events. Thermal signal absorption (attenuation of thermal signal by carbon dioxide and water vapour) impeded

detectability. Thermal scattering (there are many types of thermal scattering, i.e., elastic, Rayleigh, Mie, which also cause signal attenuation or signal noise) contributed to the large number of false positives (see Havens and Sharp (2016) for a thorough review). Lunar illumination during the full moon and lunar reflection (in combination with other features such as water in cattle hoof imprints) were also perceived contributors to false positives. False positives could also have been the result of error in GPS positions. When investigating the recorded coordinates, the drone GPS error and error arising from position calculations by the TagPilot software were compounded with error of the handheld GPS unit used during ground verification. For example, none of the nests located on the ground were precisely at the GPS location provided by the drone (observed range was a minimum of 2 m to a maximum of 10 m). It is also worth noting that some of our false positives were likely nests, but we were unable to locate them during ground surveys.

Secondly, we found that detection of individual nests varied between sample nights, for example, some nests were detected every night, but others were only detected a single night. Although at most sites all, or the majority, of known nests found using traditional methods were also located using the drone, multiple nights were required to achieve the totals presented. It is unclear what might account for the variation in thermal visibility; it could be that the thermal signal was present but missed because of background thermal signals, or problems with sensor sensitivity, or the thermal signal was attenuated by microclimate and habitat or macro influences. We observed adult females at numerous sites as a silhouette against the nest bowl and we suspect, based on field observations, that the outer feathers of the female were often close to thermal equilibrium with the background. At low altitude most of the thermal signal originates from the nest bowl and the eggs within rather than the adult bird. The apparent temperature of the female thermal target based on the research by Best and Fowler (1981) and the average ambient

temperature during the survey (10.33º C) would equal 13.25ºC. Thus, positive nest detection might be strongly influenced by exposure of the nest bowl and perhaps by the close attendance of the female to the nest.

In response to microclimate and habitat, and macro influences we summarized potential strategies to mitigate the challenges. Nest sampling occurs in a very short period each year, and completely avoiding extreme weather and lunar cycles (i.e., only operating under a new moon) or limiting sampling to a small window near sunrise is not practical. Potential mitigation strategies include lowering altitude to investigate a thermal signal to aid in target identification. Reducing thermal scattering and reflection effects can be mitigated by using viewing-angles close to nadir. Havens and Sharp (2016) suggested that at angles greater than 45º, signal attenuation, and thermal scattering impede the ability to accurately detect thermal signals. As other research suggests (Garner et. al 1995, Gonzalez et al. 2016, Havens and Sharp 2016), sampling after thermal equilibrium is reached (sampling pre-dawn to shortly after sunrise) can partially mitigate signal attenuation and false positives associated with microclimate and habitat influences, thus increasing detectability but is limited in duration. We found that nests were easier to detect closer to sunrise (suggesting that thermal equilibrium had been reached), although this time-period also coincides with microclimatic challenges such as the formation of morning radiation fog. Sources of GPS error can be mitigated by using a differential drone and handheld GPS system to increase positioning accuracy to under 1 m. To accurately assess false positives and increase nest detections, precise GPS coordinates (sub meter) are required; commercially available drones now have positional error to centimeter-level precision. Future research should address detectability of nests as a function of weather, atmospheric conditions, and other factors to determine optimal survey periods to increase detectability.

The point-transect survey method using the drone took 2.5–5 times longer at the upland sites in this study than a traditional chain drag method (J. Brice, Delta Waterfowl Foundation, personal communication). It is important to note that the point transect method was chosen in part because of software flight planning constraints. The survey software used in our study (Tag Pilot) did not have a means to preprogram the transect points, and therefore we manually programmed waypoints into an alternate program for flight reference. Software more recently available from DJI displays the GPS position of the drone (eliminates the need for Tag Pilot) and allows for semi-automated grid and transect planning with more granular control of flight execution. Automated or semi-automated continuous transect or grid flight sampling reduces sample time, so this constraint has already been eliminated. Additionally, automatic detection of the targets would also reduce sampling time. In two multirotor drone studies (Longmore et al. 2017, Seymour et al. 2017) using similar flight planning to our study but with fully automated detection, the researchers were able to identify large mammal species. Developing effective automated drone sampling coupled with automated detection for smaller targets such as avian nests should be a goal of technical research in drone applications.

MANAGEMENT IMPLICATIONS

We found that a point transect survey using a drone with a thermal camera can find nests of a variety of avian species across a range of habitats. Although sample size was low, most of the known nests located using traditional ground search methods were located using the drone. The large number of false-positive thermal signatures and signal attenuation that were encountered in the field from microclimate, habitat, and macro influences, was unanticipated during survey planning. Since all practitioners would ideally like large sample sizes and few false positives, we

propose several mitigation strategies. Drone technology as show here has potential applications in avian nest searching, and many managers are keen to adopt these tools. However, if this technology is to be practically applied as a standard nest-census tool, and ideally automated to reduce sample time and increase the total area sampled, future research should address the large number of false positives and explore methods to mitigate them.

Chapter 3 – Upland Waterfowl Nest Searching – A Comparison Between Methods and Factors Influencing Drone Detection

FOREWARD

This chapter builds on the previous in so that we examine the comparison between the drone and traditional nest searching for upland waterfowl in greater detail. We designed this study to test a commercially available drone and thermal camera for a practical, over-the-counter drone nest searching application to be used by biologists in the field. This approach aimed to identify thermal targets in real-time that we investigated following the drone flights. It explicitly addresses Objectives 2 and 3 of the Thesis. Firstly, we compare the two methods, only including variables common to both. Secondly, we examine the drone method independently and consider additional variables influencing detection.

INTRODUCTION

Nesting studies are an essential tool for understanding waterfowl ecology. Nesting studies provide insights into the quality of the nesting habitat by evaluating the productivity of waterfowl habitat (Miller and Johnson 1978). Nest success is one of the essential vital rates used to estimate waterfowl production and population dynamics (Hoekman et al. 2002, Koons et al. 2014). Waterfowl management is influenced at international (e.g. North American Waterfowl Management Plan) and regional scales (Williams et al. 1999) by vital rates such as nest success. The Prairie Pothole Region is critical because it accounts for more than 50% of North America's waterfowl production (Doherty et al. 2018). Prairie Habitat Joint Venture develops an Implementation Plan approximately every five years in which they use multi-year nesting study

sites to model the impact of predicted habitat change on duck productivity. The models identify core breeding areas, which guides waterfowl habitat conservation, restoration, and enhancement planning to deliver programming in areas with the highest impacts (PHJV, 2021).

Higgins et al. (1969) first published a manuscript describing a waterfowl nest searching technique using a cable dragged behind two vehicles. The method had significant advantages (i.e. the capacity to search large areas in various habitat types) comparted to other techniques used at the time. In 1977 the construction of the cable-chain was detailed (Higgins et al. 1977), and in 1986 a standardized nest searching manual was developed (Klett et al. 1986). For over 30 years, the method outlined by Klett et al. (1986) has been the standard nest searching technique used for most upland waterfowl studies, which can collect large sample sizes economically and efficiently.

The use of drones to study wildlife has rapidly increased over the last two decades as this primarily military technology saw civilian adoption. Early studies (Leon 1997, Lee 2004) saw the potential of drones to be adopted by wildlife practitioners as a safer alternative with lower costs and increased access compared to traditional aerial surveys to study wildlife. In 2016 Delta Waterfowl Foundation field-tested a drone with a thermal camera to locate upland nests. At the time, no other studies investigated thermal drones as an upland waterfowl nest searching tool nor compared the method to the traditional chain drag method. Today, drone research is widespread, and an increasing number of studies include using thermal camera technology as a nest searching tool (Bushaw et al. 2020*a*, Helvey et al. 2020*a*, Scholten et al. 2019, Sherwring and Vafdis 2021, Stander et al. 2021). However, none compare the efficacy of the method to upland waterfowl chain drags at the scale of this study and examine the influence of weather on drone detection rates.

OBJECTIVES

The objectives of this study are:

1) To compare the efficacy of a commercially available drone with a thermal camera to the traditional chain drag method in locating waterfowl nests.
2) Examine meteorological conditions' impacts on the thermal drone method detection rates of upland waterfowl nests.

To accomplish the objectives, we propose the following hypotheses based on earlier research recommendations (Stander et al. 2021), our understanding of thermography, and the weather's influences on detection. First, we predict that the drone method will find more nests and have higher detection probabilities of incubating nests than the chain drag method. Specific to factors that influence the drone method detection, secondly, we predict that higher humidity levels will decrease detection rates, lower ambient temperatures will result in increased detection rates, more nests will be found closer to sunrise, and denser cover will decrease detection rates.

STUDY AREA

We conducted upland waterfowl nesting surveys in Benson, Cavalier, and Towner counties of North Dakota, USA, (Fig. 3.1) by Delta Waterfowl Foundation (hereafter Delta) research staff from 8 May to 15 June 2018. The topography of the study area is characterized by the gently rolling landscape typical of the Central Lowlands in the Prairie Pothole Region. Historically, the area was dominated by mixed-grass prairie and high densities of interspersed glacially formed wetlands, much of which was altered to support agricultural production (Doherty et al. 2018, Kantrud et al. 1989). We selected nest searching sample sites based on historically high waterfowl nesting densities, high breeding pair densities, and high-quality nesting areas with the assistance

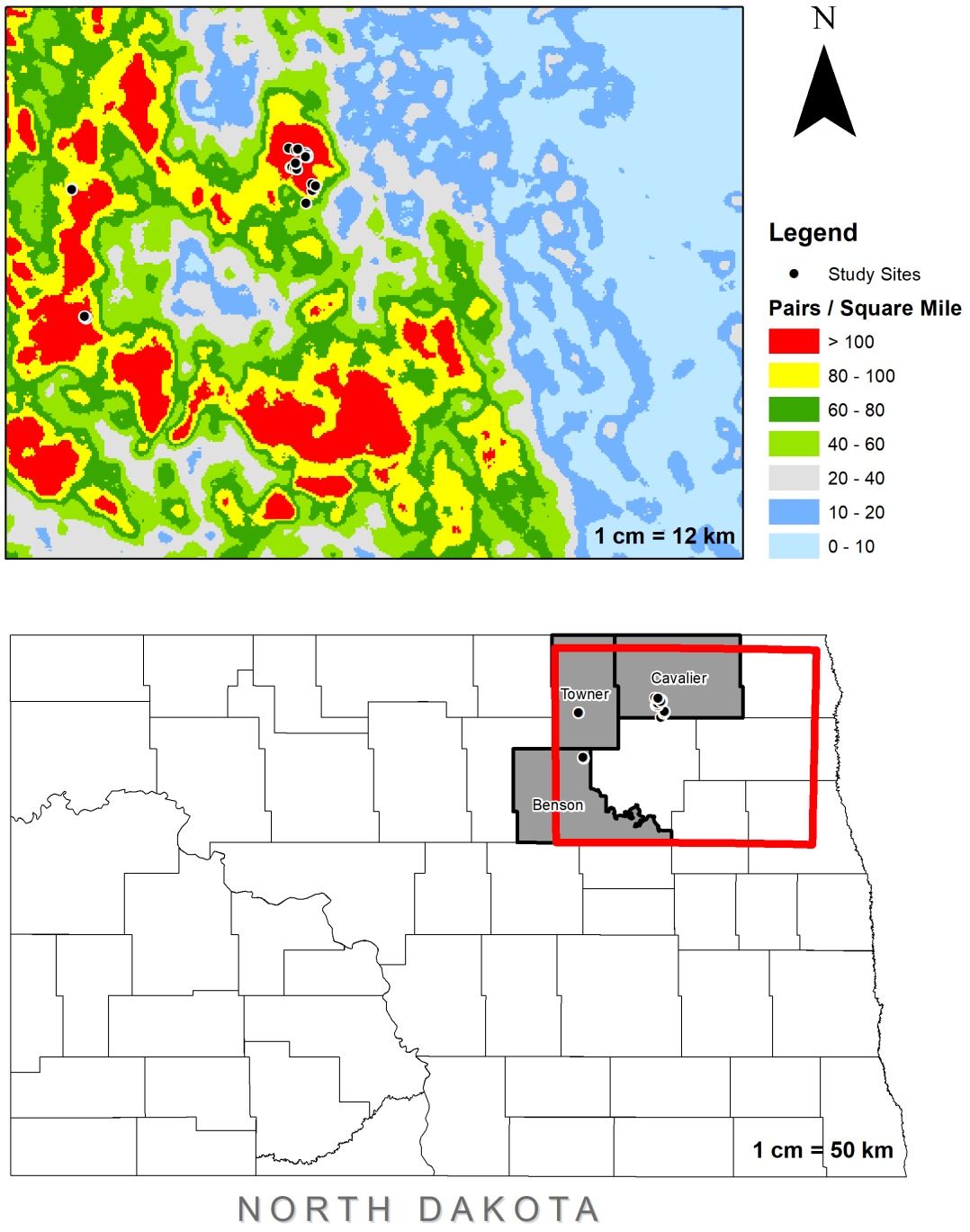

Figure 3.1. General study area showing study sites in Benson, Cavalier, and Towner counties, ND, USA, with waterfowl breeding pair densities from Four Square Mile Survey (USFWS 2012).

of United States Fish and Wildlife staff (Fig. 3.1). In total, we surveyed 24 sample sites ranging in size between 9 ha – 15 ha. We maintained a minimum 100 m buffer between sites. Figure 3.2 shows an example of multiple sample sites within the same quarter section of land.

Figure 3.2. Example of two sample sites within a single quarter section ranging in size from 10 – 12.5 ha in Benson, ND.

Weather data for Devil's Lake, ND, during the survey period is summarized in the appendix Table A, and we show long-term average monthly temperatures and precipitation in Table 3.1. During the survey, sunrise ranged from 0606 hours (8 May) to 0534 hours (15 June), and sunset ranged between 2102 hours and 2141 hours, respectively.

Table 3.1. Long-term average weather data in Devil's Lake, ND. Retrieved from weather station WBAN:94928 (NOAA, 2022).

Month	LTA Monthly Temperature (°C)	LTA Monthly Precipitation (mm)
May	13.3	62.74
June	18.2	101.85

METHODS

Drone nest searching

Drone Specifics and Thermal Target Identification

We adapted drone nest searching methods following recommendations from Stander et al. (2021). We used a rotary-wing Inspire 1 model T600 drone (DJI, Shenzhen, China). The LiPo 6S (TB48) battery-powered drone weighs approximately 3.2 kg with the Zenmuse XT 19mm (DJI, Shenzhen, China) thermal camera payload and is 438x451x301 mm in size. We conducted drone nest searching surveys between 0123 hours ($\bar{x}$=0204 hours, SD=0031 hours) and 0640 hours ($\bar{x}$=0514 hours, SD=0053 hours). We launched and landed the drone with no specialized equipment in weather conditions free of heavy fog or rain because the drone equipment was not waterproof, thermal detectability was impaired, and we had to avoid low cloud ceilings (<173 m) due to federal drone laws.

The survey polygons were pre-programmed using QGIS (QGIS.org) using satellite imagery to avoid waterbodies within sample polygons to minimize thermal interference (Stander et al. 2021) and uploaded to the Ground Station Pro app (DJI, Shenzhen, China) used to control the drone during the flights. We programmed transects with 30 percent side image overlap and 40 percent front image overlap (optimal settings determined during field testing for full coverage and

flight efficiency). Once we increased altitude to 51 m – 54 m above ground level (agl) the preprogrammed transect flight of multiple waypoints was initiated (Fig. 3.3). At survey altitude, the ground sampling distance (GSD) ranges between 4.6±0.2cm – 4.8±0.2cm. We flew the drone with the camera orientated 90° to the flight path (pointed straight down).

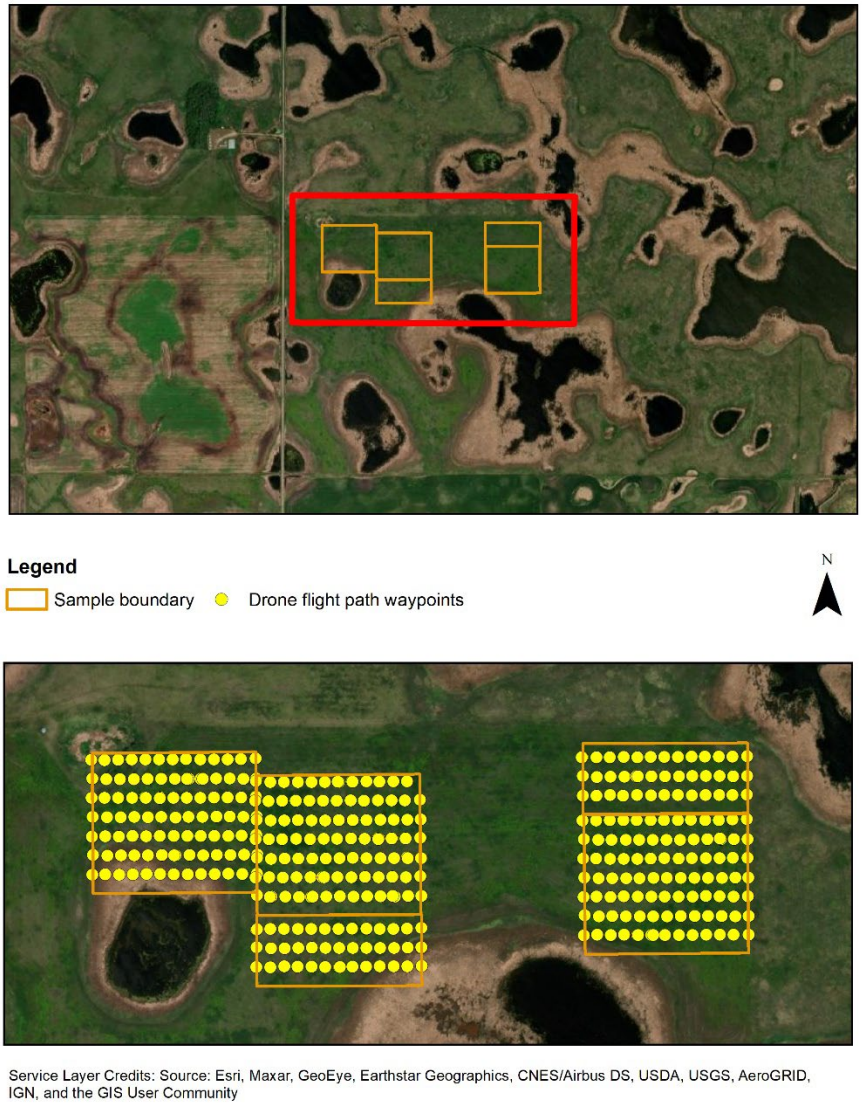

Figure 3.3. Example of sample boundary and drone flight path waypoints.

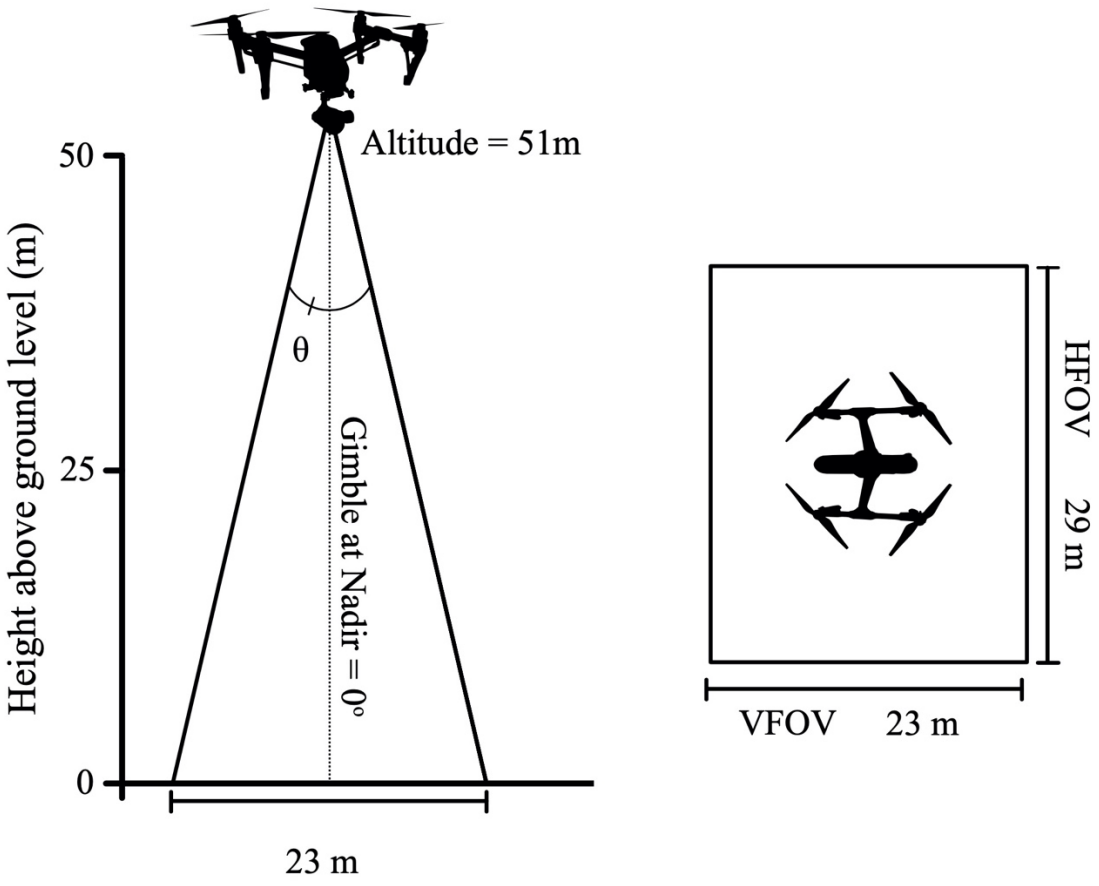

Figure 3.4. Thermal camera footprint at 51 m agl and gimbal (camera) angle.

operating the camera at nadir provides a constant viewing angle, minimizing duplicate search areas and increasing the probability of detection due to decreases of thermal reflections from non-targets resulting in increased clutter and noise, which can cause false positive signals (Havens and Sharp 2016, Stander et al. 2021).

When we observed a thermal target of interest, we paused the flight and slowly decreased the drone altitude until we classified the thermal target into three categories: 1) a nest, 2) a nest-like target, or 3) rejected as a false positive signal. If we did not dismiss the target as a false

positive, we recorded the GPS coordinates of the target when hovering the drone directly over the center of the thermal target. After recording the location, we slowly increased the drone altitude and resumed the preprogrammed transect flight from the last waypoint. After the sample site survey, we transferred the recorded GPS coordinates to the handheld Garmin 64s GPS (Garmin LTD, Canton of Schaffhausen, Switzerland) for ground verification. Delta Waterfowl Foundation implemented nest searching and monitoring under scientific collection permit GNF04647842 with the North Dakota Game and Fish.

Drone Ground Verification

Drone target ground verification typically occurred the same morning or up to three days following the drone searches in cases where inclement weather and associated risk of female nest abandonment prevented ground verification. We conducted visual nest searches at each GPS coordinate. We expected a maximum GPS of 10 m (based on 2017 testing) and focused our searches within a 10 m radius of the GPS coordinate. We anchored a rope at the GPS location and searched in concentric circles 2 m apart. The search area was visually inspected for signs of a duck nest with at least one egg present with the aid of nest searching sticks to search underneath vegetation. If no duck nest was present within the 10 m search radius, we disregarded it as a false positive. If we discovered a duck nest, we proceeded to measure and determine the characteristics of the nest and its surroundings. We recorded the location of the nest using the GPS waypoint averaging function. We measured the distance between the drone GPS coordinate and the nest to the nearest 0.1 m. We used visual obstruction readings (VOR) to estimate average vegetation height with a Robel pole following methods outlined by Robel et al. (1970). We classified vegetation types around the nest into categories (bare ground; forbs; grass; and litter to sum to 100

percent using a 50 cm x 50 cm Daubenmire frame (Fig. 3.5) following methods by Daubenmire

Figure 3.5. Depiction of ground verification nest measurements showing vegetation categorization using the Daubenmire frame.

(1950). We determined the nest species by observing the female flush (if present), egg identification or observing the female on subsequent nest monitoring visits. We measured clutch size, incubation category (laying or incubating), and egg viability by field candling (Weller 1956). We marked the nest with a 40 cm long, 5 mm thick wire with approximately 5 cm of the tip spray-painted orange (the wire markers were only visible within close proximity of the nest). We covered the nests with vegetation and down (if present) and placed blades of grass in an x pattern to determine if the female had revisited the nest before the subsequent chain drag as an indicator of nest activity status.

Weather Data Collection

We collected local weather data (barometric pressure, dewpoint, humidity, and temperature) during the drone flights by placing a Kestrel 5500L portable weather station (Kestrel Meters, Boothwyn, PA) 5 m north of the drone take-off location. We used the Kestrel weather data associated with the time when we first observed the thermal signal. For nests not located using the drone method (i.e. only found using the chain drag method), we overlapped the drone GPS flight log and nest GPS coordinates to determine the timestamp the drone flew directly overhead the nest. We spatially cross-referenced the flight log waypoints with missed nest locations and recorded the associated time the drone was overhead.

Upland Chain drags

We conducted chain drag nest searching surveys 1 – 4 days following drone ground verifications between 0735 hours ($\bar{x}$=0905 hours, SD=0104 hours) and 1400 hours ($\bar{x}$=1051 hours, SD=0104 hours). Search area polygons were programmed into the handheld GPS unit to ensure complete coverage of the search area. We searched for nests by dragging a 30 m 0.8 cm diameter chain between two all-terrain vehicles following methods outlined by Gloutney et al. (1993), Higgins et al. (1969), and Klett et al. (1986). We searched the area for 10 minutes when we observed a female flush. When we found a nest, we noted if it was also previously located during the drone ground verification, recorded biological covariates (incubation stage and clutch size), and covered the nest. In addition, we measured Visual Obstruction Reading (VOR), determined vegetation classification, and recorded the averaged GPS location when we discovered a new nest. Afterward, we covered the nest with nesting material and marked it with an x. When we completed the survey, we revisited any nests located during drone ground verifications that we missed using the chain

drag method. We investigated the missed nests for signs that a female had returned to the nest since the last visit (drone verification), and we determined if the nest was still active. If the female abandoned the nest, we removed the data point from the entire sample.

Data Analysis

Comparison of Nest Searching Methods Analysis

We used a Huggins' closed capture model (Huggins 1989) in Program MARK (ver. 9.0; White and Burnham 1999) to estimate nest detection probabilities for both methods. The model assumes that the population is closed, i.e. that the nests are detectable for both the drone and chain drag methods. We assumed that there was no behavioural response for females encountered during the drone ground verification, i.e. any interaction with females during drone ground verification did not influence (i.e. increase or decrease the likelihood) chain drag method detection. We, therefore, constrained capture probability (p) to equal the recapture probability (c) for the two methods (Moore et al. 2004). We created a two-encounter history for each nest, with drone encounters coded as the first occasion and the chain drag method as the second occasion. The binary data produced three potential encounter histories, x_{10} if the nest we only detected using the drone method, x_{01} if the nest was only detected by the chain drag method, or x_{11} if both methods detected the nest. We evaluated the fit of each model using Akaike's Information Criterion (AICc; Burnham and Anderson 2002), which we corrected for small sample sizes. To compare detection probabilities, the 9 models evaluated only included covariates that we identified could influence both methods independently (Table 3.2). We defined incubating nests as those determined by candling at ≥1 day incubation. For the analysis, we adjusted clutch size (egg.no) and incubation

stage (of incubating nests) to account for the time between the drone and chain drag surveys. We subtracted the number of days post the drone survey with the assumption that females lay one egg each day or incubation progresses linearly. We also considered simpler models wherein we reduced the incubation category (inc_cat) to incubating or laying stage (inc_cat_reduced).

Table 3.2. Covariates used in Huggins' closed capture model to compare drone method to traditional chain drag method for upland waterfowl nest searching.

Variable	Description	$\bar{x}$	Range
egg.no	Clutch size (adjusted to day of drone flight)	8.2	1 – 12
forbs	% forbs within 50 cm^2 of nest bowl	13.7	0 – 75
inc_cat	Incubation stage (adjusted to day of drone flight). 0 = not incubating; 1 = early incubation (1 – 13 days); 2 = late incubation (14 – 22 days)	0.7	0, 1, or 2
inc_cat_reduced	Incubation stage reclassified as either in laying stage or incubating	0.6	0 or 1
j.date	Julian date when we found the nest	150	126 – 166
log.vor	Log values of visual obstruction readings	1.19	0.90 – 1.55

Drone Specific Analysis

We analyzed the importance of covariates contributing to the detection of duck nests by the drone method using a multiple binary logistic regression (BLR) model implemented using the generalized linear model function ("glm") in CRAN R (R Core Team 2018). The probability of the drone detecting a duck nest using linear regression was estimated by:

$$logit\ (D_s) = \beta_0 + \beta_1 X_{1,s} + \cdots \beta_k X_{k,s}$$

where logit *(D)* = logit transformed estimate of detection during a drone survey *s*, $\beta_0 \ldots \beta_k$ is a series of estimated logistic regression coefficients, and $X_1 \ldots X_k$ are observed covariate values from each survey.

We chose to fit a single *a priori* model that assessed the primary objective by including covariates that have been shown to influence the effectiveness of thermal camera technology at detecting thermal signatures. Included in the model were covariates related to the specific survey, such as Julian date and minutes since midnight (i.e., 12:00 pm, 0000 hours). We included weather-related covariates like relative barometric pressure (mbar), dew point (Celsius), humidity (%), temperature (Celsius), and the difference between temperature and dew point. Lastly, characteristics of the duck nests were considered, such as species, incubation category, and VOR. Because we measured most weather covariates on different scales that varied widely, we decided to normalize these covariates so that individual covariate contributions would not create bias during model fitting (Table 3.3). We used a "minmax" scaling equation to transform all values to a range of 0-1 given data distributions were not bell-shaped in appearance. The min-max scaling equation subtracts the overall minimum covariate value from the observed covariate value (V_o), then divides that value by the full range of the covariate of interest.

Table 3.3. BLR model covariates evaluated for the drone specific analysis.

Covariate	Unit	Min	Mean	Max	SD
Dew point	ºC	-6.9	10.5	15.9	4.2
Barometric pressure	mBar	948.7	958.5	968.4	5.9
Temperature	ºC	-1.0	13.5	18.1	3.5
Relative humidity	%	54.0	82.6	99.2	10.3
Time (min. after 0000 hours)	min	101.0	236.7	373.0	64.8
VOR (logarithmic scale)	n/a	0.9	1.2	1.6	0.1
Temperature - Dew Point Difference	ºC	0.1	3.0	9.0	1.9
Clutch size	eggs	2.0	9.0	13.0	2.2
Julian Date	days	130.0	151.0	165.0	8.8

$$\frac{V_o - V_{min}}{V_{max} - V_{min}}$$

When logical, we tested for non-linear effects of covariates and used Akiake's Information Criterion adjusted for small sample size to determine if non-linear terms should be included. Non-linear inclusion required an improvement in model performance indicated by a ≥2 point reduction in AIC_c. Lastly, we removed outliers from the data (n = 4), omitted non-independent covariates from being included in the a priori model, and assessed the multicollinearity of the remaining covariates using Pearson's correlation criteria to ensure assumptions of a multiple logistic regression approach were not violated.

RESULTS

In total, we identified 150 nests from five species, including 52 blue-winged teal (*Anas discors*), 33 gadwall (*A. strepera*), 28 mallard (*A. platyrhynchos*), 26 northern shoveler (*A. clypeata*), and 11 northern pintail (*A. acuta*) using both methods.

Comparison of Nest Searching Methods (Huggins' closed capture model)

Proportionally out of the total sample, 21% (n=32) were detected only by the drone method, 51% (n=76) were detected only by the chain drag method, and both methods detected 28% (n=42). The detection probability of the null model for the drone method is 0.36±0.04 and 0.57±0.06 for the chain drag method. We tested several models and ranked them based on differences (Δ) in AIC_c score (Table 3.4). The top four ranked models included incubation category (inc_cat_reduced or inc_cat) as a covariate. However, a high degree of uncertainty is associated with laying stage nest detection estimates from the models that include incubation category as a covariate due to the small sample size of laying stage nests found using the drone method (Table 3.5) and because we determined that immigrating females violate the closure assumption of the models (expanded on in discussion section). Consequently, the most parsimonious model that does not violate underlying assumptions is p(Method + egg.no) = c(.) and has an AIC_c value of 305.23. Detection

Table 3.4. Best fitting models for comparison of detection rates between drone and chain drag methods ranked by differences Akaike's Information Criterion scores corrected for small sample sizes (ΔAICc).

Model	AIC_c	Delta AIC_c	Model Likelihood	Num. Par	Deviance
{p(Method + inc_cat_reduced) = c(.)}	217.62	0	1	3	211.54
{p(Method + inc_cat_reduced + log.vor) = c(.)}	219.66	2.04	0.36	4	211.53
{p(Method + inc_cat) = c(.)}	220.21	2.58	0.27	5	210.00
{p(Method + inc_cat + log.vor) = c(.)}	222.29	4.66	0.10	6	210.00
{p(Method + egg.no) = c(.)}	305.23	87.60	0	3	299.15
{p(Method + log.vor) = c(.)}	311.95	94.33	0	3	305.87
{p(Method) = c(.)}	313.19	95.56	0	2	309.15
{p(Method + j.date) = c(.)}	313.39	95.76	0	3	307.31
{p(Method + forbs) = c(.)}	314.68	97.06	0	3	308.60

Table 3.5. Incubation stages of nests detected by both methods.

Method	Total Nests	Laying stage	Early Incubation[1]	Late Incubation[2]	Total Incubating
Drone Method	74	2	61	11	72
Chain drag Method	118	56	52	10	62
Total	150	58	79	13	92

[1] 1-12 days incubation. [2] 13 - 22 days incubation

estimages for both the drone method (Fig. 3.6) and the chain drag method (Fig. 3.7) trend upward with increasing clutch size. We detected 2 unique (only found using drone method) laying stage nests using the drone method as shown in the raw nest detection values in Table 3.5, which we found at 0322 hours and 0427 hours

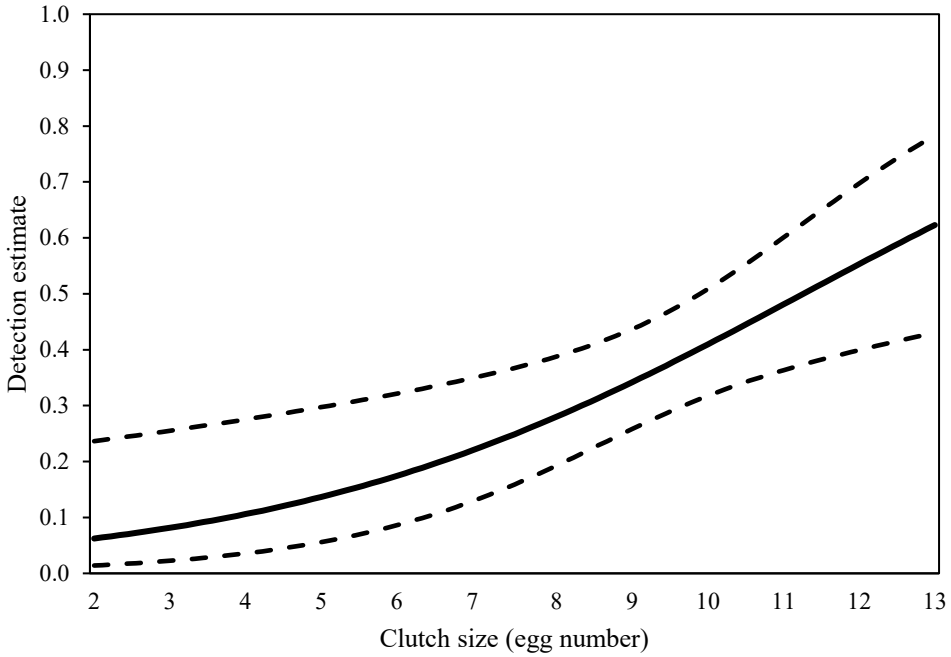

Figure 3.6. Estimated drone method nest detection as a function of nest clutch size.

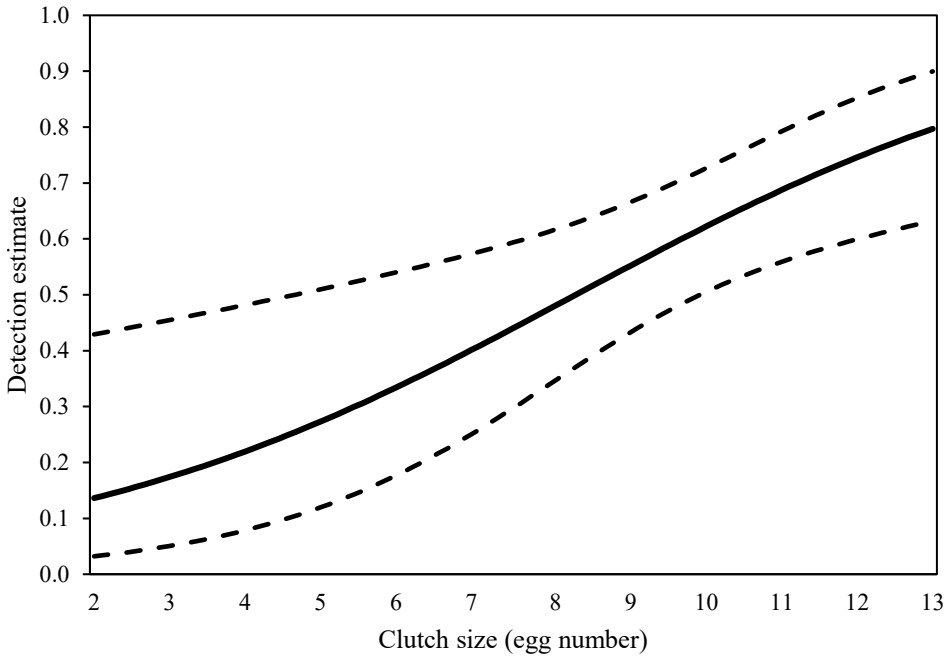

Figure 3.7. Estimated chain drag method nest detection as a function of nest clutch size.

(Fig. 3.8). We detected 56 laying stage nests using the chain drag method with most detections between 0900 hours and 1000 hours (Fig. 3.9). Due to the large difference in laying stage nest detections we suggest that the drone method is ineffective at finding laying stage nests during the survey period. We hypothesised that the drone method would have higher detection rates for incubating nests, but we are unable to statistically test this due to low sample size and model violations. Again, using mallards as a benchmark, at the average incubated clutch size 8.9±1.67 (Arnold et al. 2002), the estimated detection probabilities for both drone method are 0.27±0.05 – 0.44±0.06 and for the chain drag method are 0.42±0.08 – 0.65±0.06.

Time duration for drone nest searching averaged 185 min/site (SD=47 min) and drone ground verifications averaged 71 min/site (SD=62 min). No times were deducted for nest measurements (VOR estimates and vegetation classification), which we did not repeat if we

relocated a nest using the chain drag method. Chain drag surveys took an average of 105 min/site (SD=63 min) and included the time required to complete nest measurements for nests not found by the drone method.

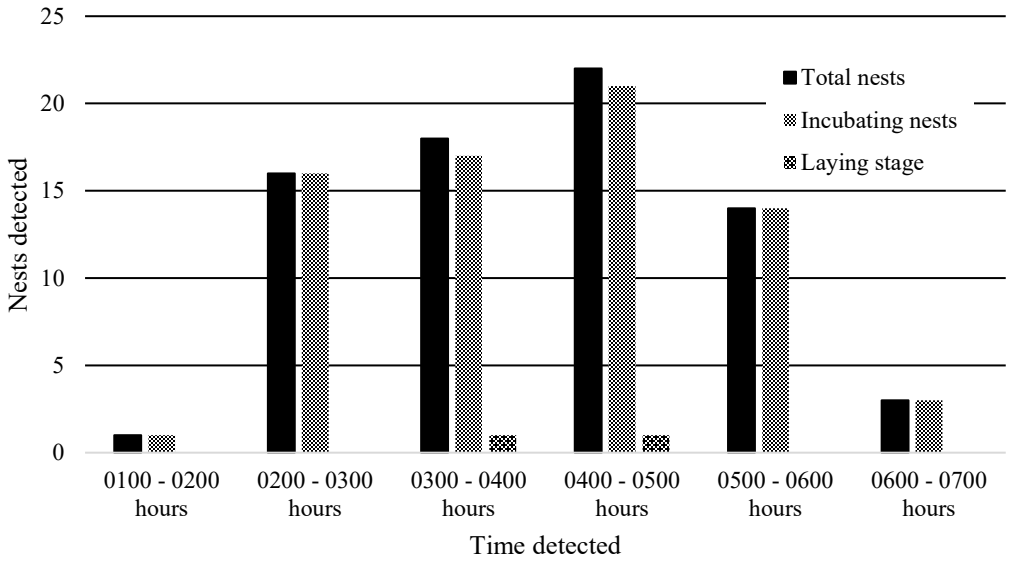

Figure 3.8. Nest detection times between 0100 hours and 0700 hours for incubating and laying stage nests using the drone method.

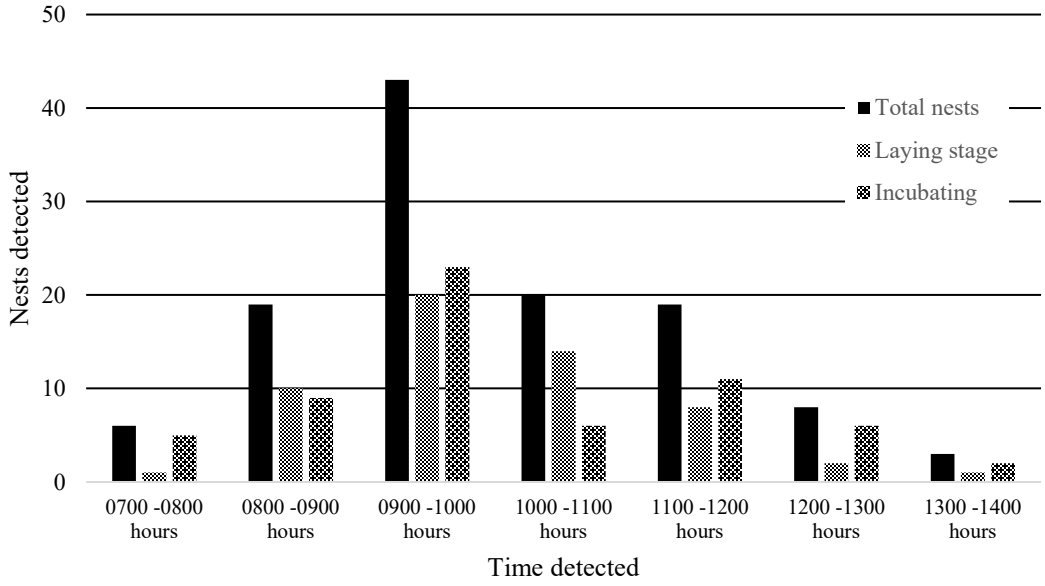

Figure 3.9. Nest detection times between 0700 hours and 1400 hours for incubating and laying stage nests detected using the chain drag method.

Drone Specific Results

We included several weather related, temporal, habitat, and biological covariates to test our drone-specific hypothesis. During exploratory data analysis, we found that many of the weather covariates were correlated. Physical principles can account for several of these relationships. For instance, there is a correlation between relative humidity, dew point, and barometric pressure. It was observed that incorporating deviations from these relationships, such as the normalized difference between temperature and dew point, improved the model's performance (overall lower AIC), although the model was not significant ($p > 0.8$). We selected the correlated variables that enhanced the model's performance, while we excluding variables like species or ambient temperature, that did not contribute to performance. The best model had an AIC score of 119.57 and included the covariates shown in Table 3.6. The results indicate that incubation category is

the most significant positive predictor of drone method nest detection ($p < 0.001$).

There is a non-linear trend between Julian date and barometric pressure. Although Julian date is not a significant predictor of nest detection ($p > 0.1$), the data (Fig. 3.10) shows a trend that the ratio between detections and non-detections for the drone method was consistent throughout the sample period except for two distinct periods. We refer to the two periods as case studies hereafter. The Julian dates are 143 – 147 for case study A (low drone detection) and 158 – 159 for case study B (high drone detection). The following are summaries of weather observations corresponding to the case studies. During case study A, we observed low to very low contrast in the thermal drone imagery (uniform signal with few notable thermal hotspots). In one instance, after inspecting a thermal target at a low altitude (a passerine bird perched near the ground), we observed the thermal signal disappear at 20 m agl as the drone was returning to survey altitude. In addition, we observed dew on the ground and on another occation noted an apparent improvement in the thermal imagery contrast when the moon set. Specific to case study B, there were no notable observations

Table 3.6. Binary Logistic Regression Model scaled output table examining covariates influencing drone method detection rates.

Coefficients:	Estimate	Std. Error	z value	Pr(>|z|)	
(Intercept)	-11.669553	4.187277	-2.787	0.00532	**
j_date	0.264402	0.163092	1.621	0.10498	
j_date^2	-0.006419	0.003912	-1.641	0.10083	
time	0.013077	0.433514	0.03	0.97594	
diff_norm	-0.292694	1.335868	-0.219	0.82657	
baro_norm	-2.959998	3.481788	-0.85	0.39525	
baro_norm^2	7.494912	3.690144	2.031	0.04225	*
log_vor	5.080197	2.668335	1.904	0.05693	.
inc_cat1	3.911282	0.696866	5.613	1.99E-08	***

Signif. codes: 0 '***'; 0.001 '**'; 0.01 '*'; 0.05 '.'; 0.1 ' '; 1

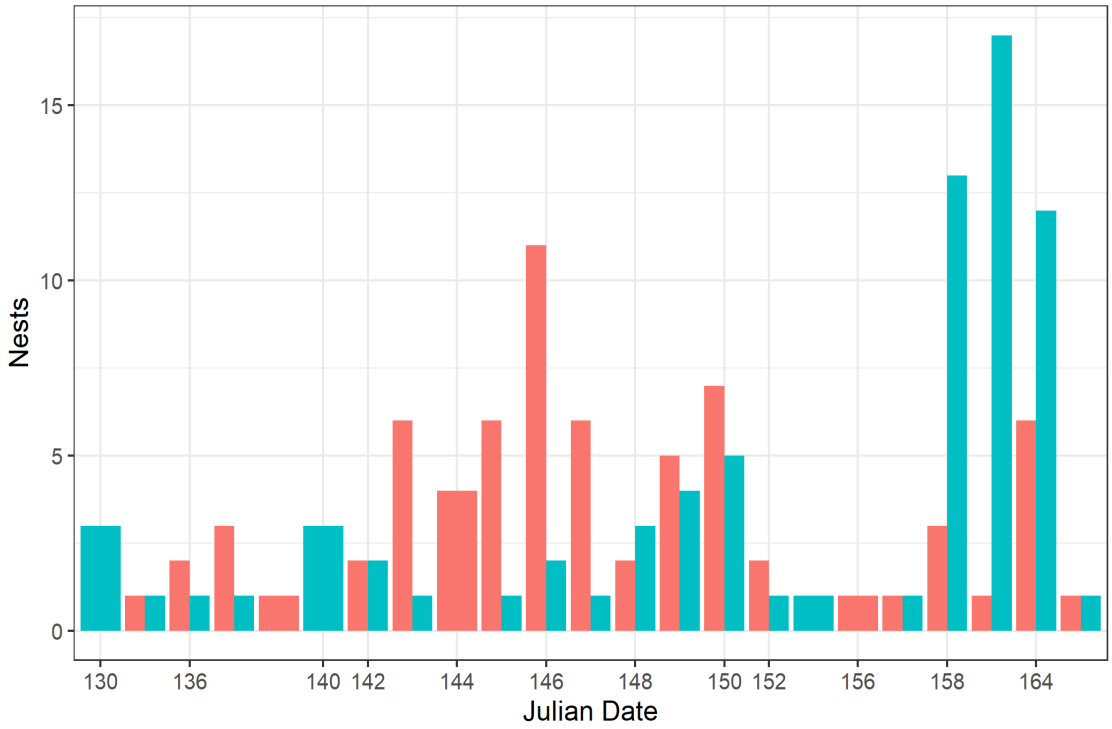

Figure 3.10. Raw drone detections and non-detections between Julian dates 130 - 164.

regarding weather, but and we observed thermal targets in over 80% of the flights compared to the 36% average of all flights. We report astronomical moon phases for each case study in Table 3.7.

Table 3.7. Astronomical conditions during two drone method case studies (TWC 2022).

Case study	Moon Phase	Rise (hours)	Set (hours)
1 (low detection)	Waxing gibbous	1448 - 1921	0326 - 0509
2 (high detection)	Waning crescent	0241 - 0546	1413 - 2129

Drone detection, represented by vegetation density (Fig. 3.11), also showed two distinct clusters of data points corresponding to the same case studies. The grassland composition of case study A was mixed, comprised mainly of Kentucky bluegrass (*Poa pratensis*), quack grass (*Elymus repens)*, with some bromegrass (*Bromus* spp*.)* and some forbs such as alfalfa (*Medicago* sativa) showing signs of management, indicative of haying (Fig 3.12). The grassland habitat of case study B was dominated by brome grass and has been left idle for more than 15 years (Fig. 3.13). To interpret and evaluate the results within this study's realistic ranges, we examine these two different case studies (low and high drone method detection).

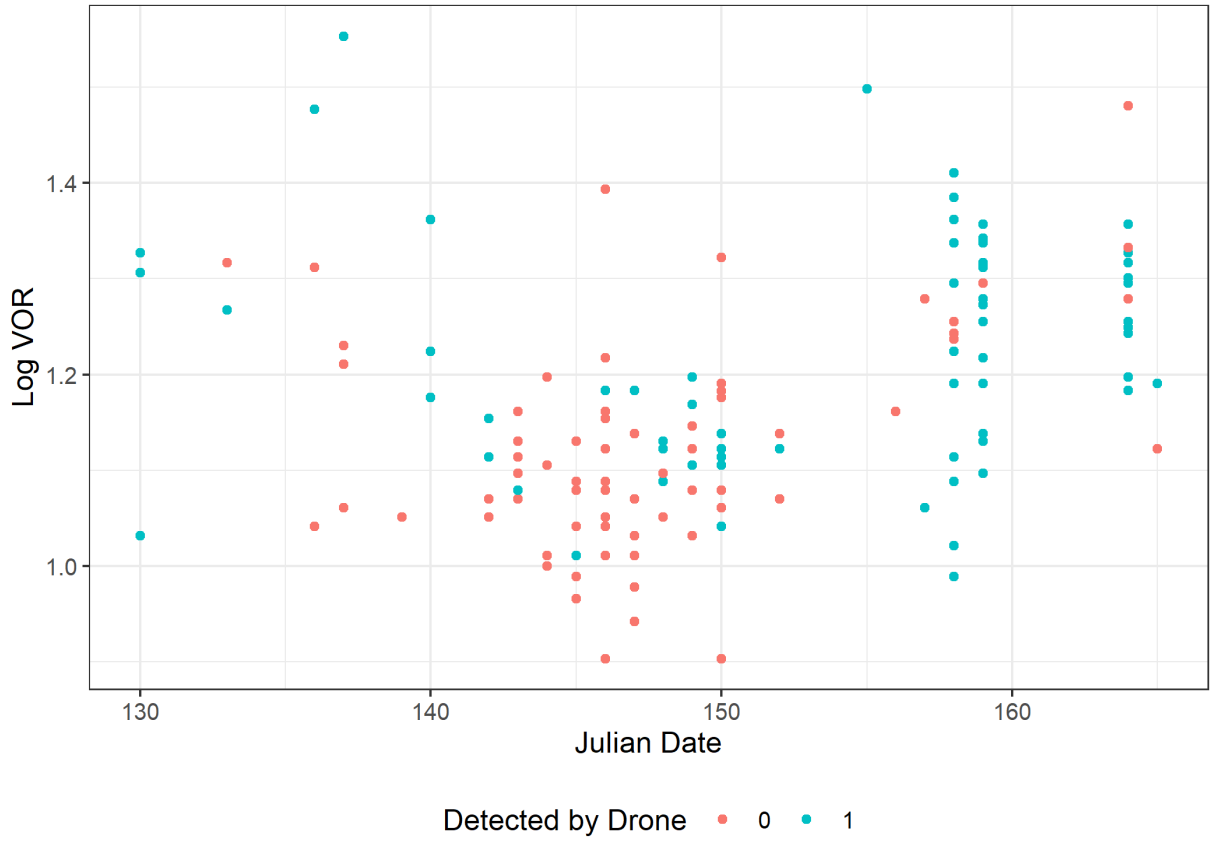

Figure 3.11. Raw logarithmic visual obstruction readings (VOR) for incubating and laying stage nests as a function of Julian date between Julian dates 130 - 164.

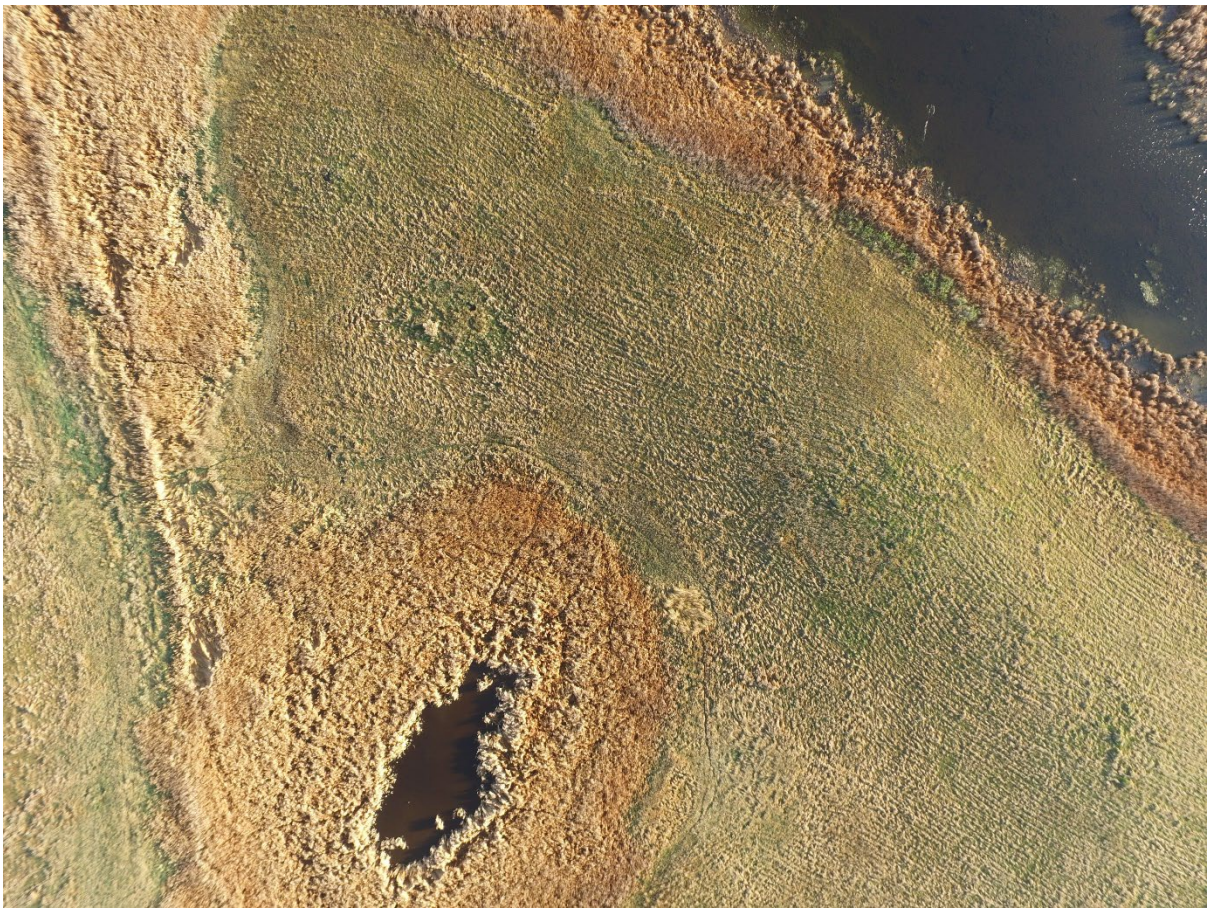

Figure 3.12. Aerial photo of sample area within case study A (low drone detection) taken at 91 m agl on 25 May 2018 in Cavalier county, ND showing signs of management.

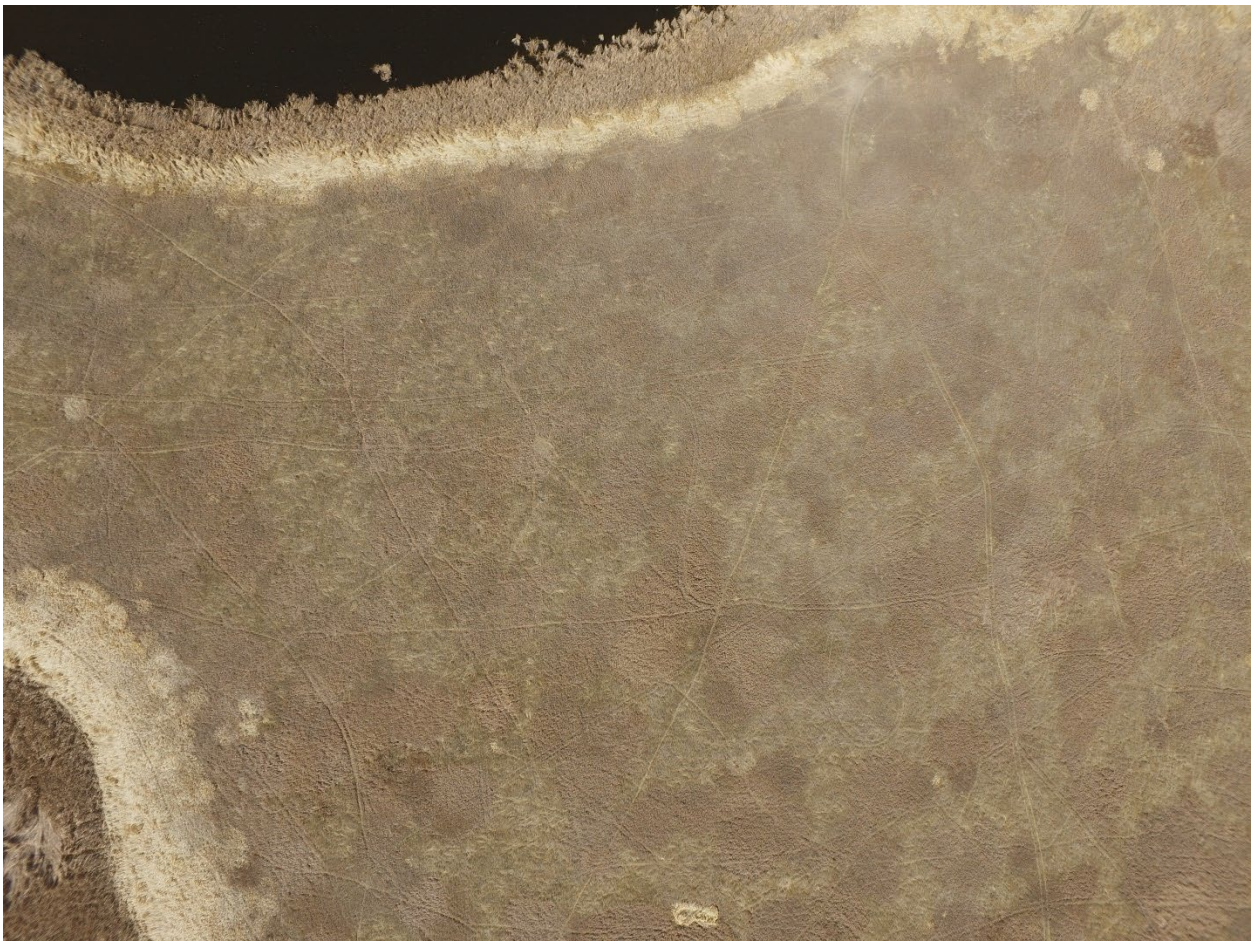

Figure 3.13. Aerial photo of sample area within case study B (high drone detection) taken at 91 m agl on 4 May 2018 in Benson county, ND, showing signs of a lack of management. ATV tracks present are from previous chain drag searches.

DISCUSSION

Our study design was limited to a two-encounter sample methodology. Our sample size of laying stage nests found using the drone method totals two nests, but we did not recapture them using the chain method. With no recapture data, detection probability using the Huggins closed capture model is inestimable because the model requires detecting marked individuals in the second capture event (Cooch 2008). Anecdotally, we found a similar number of incubating nests using

both methods, and there are apparent differences between the incubation categories. Examining factors influencing detections of laying stage and incubating nests can provide valuable insights for studies focused on either category. However, to objectively evaluate the efficacy of the drone method compared to the chain drag method, all nests should be included in the analysis. For example, the omission of laying nests can lead to biases such as underestimating nesting effort in population demographic studies, which include breeding propensity as a variable in their analysis (Miller and Johnson 1978). We identify two potential reasons for missed detections: physical absence (due to biological reasons such as incubation recesses or others) and thermal detectability (weather influences and their association with sensor sensitivity or observer error).

Although our sample size limited our ability to provide detection estimates for incubation categories (i.e. laying stage or incubating nests) using the Huggins closed capture model, the BLR model analysis presented shows that female incubation status (i.e. in laying stage or incubating) significantly impacts the drone method detection rate. Therefore, we need to consider and address the impact of drone survey methodology on nest detection, specifically, a potential relationship between the operating window that ends before 0700 hours and the underlying biology of the nesting females. If females are absent because they are on an incubation recess (Croston et al. 2020, Gloutney et al. 1993) or have not yet arrived in the morning to lay an egg during the laying stage (Loos and Rohwer 2004), the probability of detection, we presume will be zero. The eggs themselves are thermally close to the environmental background temperature, and any thermal signals are generated by the hen heating the nest bowl. In Gloutney et al. (1993), during the period of the drone method survey ($\bar{x}$ start = 0204 hours – $\bar{x}$ end = 0509 hours), the lowest mean probability of incubating female presence is above 70% for blue-winged teal and northern shoveler, and above 80% for gadwall and mallard. Their results suggest that we should expect a

high presence of incubating females, which is supported by the incubating nest detection rates shown in our results.

Considering the low number of laying stage nests detected using the drone method, research by Loos and Rowher (2004) shows that laying stage females increase nest attendance as laying progresses, but female arrival time and departure times are generally outside (> 0500 hours) the survey window of the drone method. Gloutney et al. (1993) suggest commencing nest searches at 0800 hours to reduce the possibility that a female is on an incubation break and the likelihood of locating early-laying nests prone to nest abandonment. This temporal challenge impedes detecting incubating nests using the drone method. Challenges presented by previous thermal drone research (Bushaw 2020, Helvey 2020, Shewring and Vafidis 2021, Stander et al. 2021) suggest that false positives, signal noise, weather factors, and thermal loading can impede the effectiveness of thermal cameras as time progresses after sunrise or thermal equilibrium.

The two case studies present an opportunity to examine each in greater detail. The BLR model shows a nonlinear trend between drone detection and barometric pressure (Fig. 3.14). We reviewed average barometric pressure values from the nearest weather station (Devils Lake) associated with the case study survey days and used them to calculate the predicted detection estimates based on the BLR model. The model predicted mean detection estimates of 0.23 and 0.58 for case studies A and B, respectively. Although this shows differences in detection rates, we believe that barometric pressure likely indicates presence of larger weather patterns and changes in weather. For instance, our barometric data could indicate rising or falling pressure typically associated with a coming storm or stabilizing air patterns. Indeed, 7.5 mm of precipitation accumulated in the three days before case study A, and 10.7 mm in the two days following case study B. We are also unsure if precipitation might influence female nest attendance or the thermal

properties recorded by the camera. It may be possible that nesting females could sense the falling barometric pressure before a storm (Breuner et al 2013), and that this changed their behaviour during incubation. However, the detailed weather data collection required to explore these concepts in meaningful detail is beyond the study design scope.

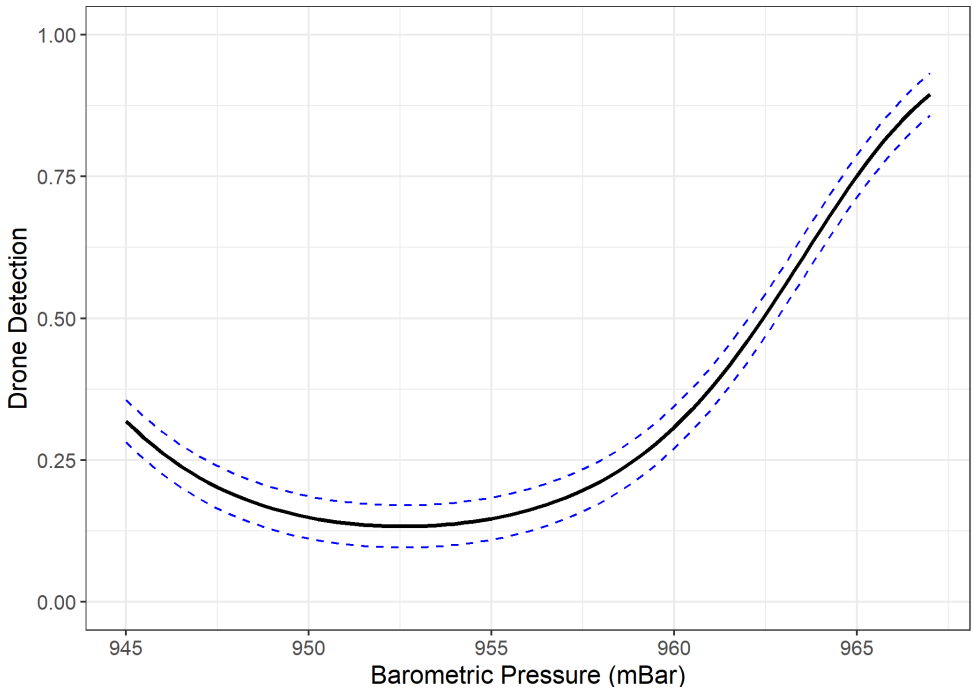

Figure 3.14. BLR model detection by barometric pressure across the range of pressures observed.

Based on Stander et al. (2021) we knew that the drone method takes longer than the chain drag to survey the same area and the study design was therefore focused on maximizing sample size. When additional time was available for surveys, we increased the sample area, and thus sampling effort. The additional time we had typically occurred when few thermal targets were observed (requiring investigation) and might have resulted in a bias toward non-detections by the drone method. It is worth noting that the drone method depends on observing a thermal target and judgement that a target is noteworthy for investigation. The study design did not consider

estimates or means to minimize observer error, which could arise from momentarily looking away from the screen or incorrectly concluding that a particular signal was a false positive. Although we measured the time required to complete each survey, the study design did not consider recording and removing the time required for nest measurements; therefore, we cannot make accurate comparisons between methods based exclusively on time. The study design did not consider other factors, such as astronomical influences noted by Stander et al. (2021). The two case studies that we identified after examining the data, had different moon phases and cyclical chronologies and may suggest that temporal autocorrelation and timing of sampling (relative to moon phase, or other phenomena) may be important in detection. Research shows that stray thermal signals emitted by the moon are detectable with a thermal camera (Montanaro et al. 2014), but we cannot make any inferences from our data about its influence.

MANAGEMENT IMPLICATIONS

We demonstrated that the thermal drone system and methodology used in this study has a lower overall detection rate for upland nesting waterfowl than the traditional chain drag method. We recommend that wildlife professionals continue to research this survey method, but as demonstrated, the drone method is not a replacement for the traditional chain drag method. Firstly, the method detected a low number of laying stage nests, and secondly, although we did not evaluate the efficiency (the sample size coverage compared to time), anecdotally, ground methods are likey still superior. We found a similar detection number of incubating nests, supporting the need for further research. The focus of the study design was to compare the efficacy of the two methods, and therefore our inferences on analysis of weather and other factors influencing thermal detection are limited. We identified incubation stage was the most influential determinant of nest detection

for the drone method. The barometric pressure was also a significant determinant of nest detection but is likely not directly influencing detection and is instead a signal or proxy for other macro weather influences that we did not consider or accurately measure.

To better understand the factors that influence the drone method nest detection, we recommend considering the following in the study design of follow-up research.

- Extend the survey period overlapping periods with higher likelihood of laying stage female nest attendance of laying stage females. However, this period will likely have more thermal interference arising from increasing landscape temperature; therefore, we recommend exploring image post-processing (Helvey et al. 2020*a*) or automated thermal image detection algorithms (Israel and Reinhard 2017, Lhoest et al. 2015) to mediate these challenges.
- Collect weather data before the survey to evaluate the influence of weather prior to and during the survey.
- Conduct repeated surveys to increase encounter history sample size for a more robust analysis. Based on anecdotal observations during the first year of sampling (Ch. 2), it may be necessary to survey with the drone three times to improve detection.
- Monitor female nest attendance to help understand why nests with females present during the survey are not detected. Consider continuously monitoring nest attendance using cellular trail camera cameras (Callery et al. 2022) adjusted for close focus and nighttime exposure (Uhe et al. 2020) to aid the discovery.

APPENDIX

Table A: Weather data in Devil's Lake, ND from May 8 – June 15 2017. Retrieved from weather station WBAN:94928 (NOAA 2022, The Weather Company 2022)

		Temperature (°C)			Dew point (°C)			Rel. Humidity %			Precipitation (mm)		Wind Speed (km/h)		Pressure (hPa)		
Date	**J. Date**	**Min**	**Avg**	**Max**	**Min**	**Avg**	**Max**	**Min**	**Avg**	**Max**	**Total**	**Min**	**Avg**	**Max**	**Min**	**Avg**	**Max**
May		**1.1**	**11.7**	**25**	**-10**	**4.3**	**12.2**	**19**	**65**	**100**	**17.5**	**0**	**21.4**	**61.2**	**951.1**	**961.3 96**	**972.3**
8	128	8.3	13.2	17.2	5.0	7.7	12.2	50	71	94	2.5	9.7	22.3	35.4	960.8	962.4	964.0
9	129	4.4	13.2	20.0	0.6	3.6	6.1	28	57	93	-	9.7	20.2	33.8	956.6	958.3	964.6
10	130	3.9	8.0	11.1	1.1	2.8	5.0	54	71	93	-	0.0	12.7	25.7	966.5	968.1	969.4
11	131	1.1	8.3	20.6	0.0	2.8	5.0	33	74	100	-	0.0	5.8	22.5	965.3	966.3	967.8
12	132	6.1	11.7	17.2	0.0	2.5	3.9	40	55	74	-	14.5	19.8	24.1	964.6	967.0	969.1
13	133	6.1	15.5	25.0	0.0	3.2	6.7	31	46	68	-	20.9	33.9	48.3	958.8	961.6	964.6
14	134	11.1	16.6	23.3	2.2	6.1	12.2	27	52	77	0.3	11.3	21.0	32.2	959.2	962.0	965.3
15	135	8.3	16.9	23.9	-2.2	1.2	5.6	19	38	66	-	0.0	11.7	17.7	957.9	962.1	965.9

16	136	10.0	12.7	16.1	5.0	9.2	11.1	53	80	94	4.3	9.7	17.3	27.4	957.5	961.2	964.0
17	137	5.0	8.8	12.2	1.1	4.9	7.2	61	78	100	-	11.3	34.9	48.3	961.1	962.6	964.6
18	138	1.1	7.4	13.9	-10.0	-4.5	1.1	22	49	82	-	12.9	24.8	33.8	961.4	963.8	968.5
19	139	2.2	9.9	15.6	-5.6	-2.4	2.2	25	46	76	-	0.0	11.7	25.7	969.1	970.9	972.0
20	140	5.0	9.5	14.4	-4.4	0.3	3.9	29	58	93	0.8	0.0	19.3	38.6	967.5	970.5	972.3
21	141	3.9	6.6	13.3	2.8	3.7	5.0	53	83	96	6.4	0.0	23.3	35.4	960.8	964.1	967.5
22	142	6.7	9.5	11.7	3.9	5.2	7.2	59	75	93	0.3	9.7	22.3	37.0	961.4	962.2	963.3
23	143	7.2	11.1	16.7	2.8	4.4	5.6	41	66	87	-	0.0	24.6	40.2	960.1	962.3	963.6
24	144	5.6	13.0	18.3	3.9	5.7	6.7	43	64	89	-	0.0	23.9	38.6	953.4	956.4	959.8
25	145	10.6	14.8	21.1	6.1	7.9	9.4	42	65	80	-	14.5	26.0	37.0	951.1	953.0	955.0
26	146	10.0	14.0	18.3	5.0	7.0	8.3	43	65	86	-	11.3	25.4	38.6	952.7	954.5	955.9
27	147	8.9	14.4	22.8	4.4	6.2	8.9	30	62	90	1.0	0.0	22.0	61.2	955.0	958.8	961.4
28	148	7.8	13.2	19.4	5.6	7.6	9.4	41	70	93	-	12.9	28.9	46.7	960.4	963.1	965.3
29	149	8.3	11.1	12.8	5.0	6.9	8.3	62	76	93	1.3	17.7	26.5	37.0	951.1	954.9	960.4
30	150	7.2	10.9	18.3	0.0	4.3	6.1	31	68	93	0.8	4.8	22.4	33.8	951.1	951.8	953.0
31	151	8.3	16.5	22.8	1.1	3.5	7.2	26	46	74	-	0.0	13.2	20.9	953.0	955.6	959.2
June		**9.4**	**19.5**	**33.3**	**1.7**	**12.1**	**18.3**	**19**	**66**	**100**	**51.3**	**0.0**	**19.5**	**51.5**	**948.6**	**959.7**	**965.9**
1	152	9.4	20.5	28.3	3.9	7.4	11.1	29	46	83	-	0.0	18.4	33.8	953.4	958.8	962.0

2	153	17.8	22.9	33.3	7.8	14.5	18.3	33	62	84	2.0	0.0	21.4	33.8	954.0	956.6	960.8
3	154	15.0	20.8	26.7	5.0	9.6	14.4	25	53	81	-	12.9	23.2	40.2	960.8	963.9	965.9
4	155	12.8	20.3	26.7	8.3	10.2	11.7	34	55	81	-	8.0	17.7	25.7	958.2	960.4	963.6
5	156	12.2	20.7	27.2	11.1	12.8	14.4	37	63	93	-	0.0	12.3	22.5	956.3	958.0	961.7
6	157	17.2	19.6	22.2	11.1	12.7	13.9	55	65	73	-	0.0	14.6	24.1	956.9	962.4	964.0
7	158	12.8	17.4	22.8	10.6	12.1	12.8	50	73	93	-	0.0	11.7	17.7	963.6	964.6	965.3
8	159	11.1	19.6	26.1	7.8	10.6	13.3	32	60	93	-	0.0	15.3	27.4	960.1	961.9	964.6
9	160	16.1	21.1	28.3	10.0	14.5	17.2	46	68	93	0.8	11.3	24.2	35.4	957.5	960.0	961.1
10	161	15.6	18.9	25.6	6.1	13.3	16.1	29	75	100	9.9	8.0	24.4	51.5	952.7	955.5	957.5
11	162	13.9	21.3	27.2	1.7	9.3	13.3	19	50	75	-	9.7	23.1	38.6	952.1	957.8	960.8
12	163	10.6	18.6	24.4	8.3	10.2	13.3	39	61	90	-	0.0	10.3	24.1	960.4	961.7	964.0
13	164	12.8	17.0	20.6	6.7	14.5	17.2	54	86	100	37.8	9.7	20.2	37.0	958.2	960.8	962.7
14	165	13.9	16.5	21.1	11.7	13.9	16.1	64	86	100	0.8	4.8	21.4	51.5	948.6	954.0	958.5
All		**1.1**	**14.6**	**33.3**	**-10.0**	**7.3**	**18.3**	**19**	**65**	**100**	**68.8**	**0.0**	**20.7**	**61.2**	**951.1**	**960.8**	**972.3**

Chapter 4 - Conclusions And Management Implications

Drone technology presents wildlife professionals with a new and novel nest searching tool to add to their toolbox. This thesis contributes to the foundational work required before adopting and implementing thermal drone methods for widespread upland nest searching. This Thesis shows proof of concept for many upland nesting species and identifies challenges associated with the method. Species-specific considerations are needed when designing thermal nest searching studies because a standardized approach for all is inappropriate. This study demonstrates that the drone and chain drag methods find similar numbers of incubating nests and that further research is needed to refine the methodology for widespread use in the Prairie Pothole Region. A more detailed investigation into the influence of weather and meteorological factors may improve detection or inform mitigations in sampling methodology to account for those influences.

The drone method has a significantly lower overall nest detection rate because limitations exist in the thermal detection of unattended upland waterfowl laying stage nests. The apparent low nest attendance of laying females during the survey period, which results in nests (and nest bowls) remaining close to ambient background temperature, precludes thermal detection of those nests using this methodology. Therefore, we strongly advocate that follow-up research considers increased overlap of the timing of drone sampling with the timing of laying stage female nest attendance. Finally, the study design does not consider the constraints required for a detailed cost analysis; therefore, we cannot report on cost efficiency, which is a critical metric for evaluating conservation value of a method. In addition to addressing the objectives, this Thesis presents standardized methodologies and recommendations for future research considerations.

LITERATURE CITED

Abd-Elrahman, A., L., Pearlstine, and F. Percival. 2005. Development of pattern recognition algorithm for automatic bird detection from unmanned aerial vehicle imagery. Surveying and Land Information Science 65:37–45.

Anderson, K., and K. J. Gaston. 2013. Lightweight unmanned aerial vehicles will revolutionize spatial ecology. Frontiers in Ecology and the Environment 11:138–146. doi:10.1890/120150.

Arnold, T., Howerter, D. W., Devries, J. H., Joynt, B. L., Emery, R. B., & Anderson, M. G. 2002. Continuous laying and clutch-size limitation in mallards. The Auk 119:261–266.

Bennett, L. J. 1938. The blue-winged teal, its ecology and management. Collegiate Press, Inc., Ames, Iowa, USA.

Best, R. G., and R. Fowler. 1981. Infrared emissivity and radiant surface temperatures of Canada and snow geese. The Journal of Wildlife Management 45:1026–1029.

Best, R. G., R. Fowler, D. Hause, and M. Wehde. 1982. Aerial thermal infrared census of Canada geese in South Dakota. Photogrammetric Engineering and Remote Sensing 48:1849–1867.

Blythe, E. M., and M. S. Boyce. 2020. Trappings of success: predator removal for duck nest survival in Alberta parklands. Diversity 12:119.

Boonstra, R., J. M. Eadie, C. J. Krebs, and S. Boutin. 1995. Limitations of far infrared thermal imaging in locating birds. Journal of Field Ornithology 66:192–198.

Boyle, M. J. 2020. The Drone Age: How Drone Technology Will Change War and Peace. Oxford University Press, New York, New York, USA.

Breuner, C. W., R. S. Sprague, S. H. Patterson, H. A. Woods. 2013. Environment, behavior and physiology: do birds use barometric pressure to predict storms? Journal of Experimental Biology 216:1982–1990. doi:10.1242/jeb.081067.

Burnham, K. P., and D. R. Anderson. 2002. Model selection and multimodel inference. Springer-Verlag, New York, New York, USA.

Bushaw, J. 2020. Applications of unmanned aerial vehicles for conducting mesocarnivore and breeding waterfowl surveys in southern Manitoba. Thesis, Louisiana State University, Baton Rouge, Louisiana, USA.

Bushaw, J. D., K. M. Ringelman, M. K. Johnson, T. Rohrer, and F.C. Rohwer. 2020*a*. Applications of an unmanned aerial vehicle and thermal-imaging camera to study ducks nesting over water. Journal of Field Ornithology 91:409-420. doi:10.1111/jofo.12346.

Callery, K. R., S. E. Schulwitz, A. R. Hunt, J. M. Winiarski, C. J. McClure, R. A. Fischer, J. A. Heath. 2022. Phenology effects on productivity and hatching-asynchrony of American kestrels (*Falco sparverius*) across a continent. Global Ecology and Conservation 36:e02124. doi: 10.1016/j.gecco.2022.e02124

Chabot, D. 2018. Trends in drone research and applications as the Journal of Unmanned Vehicle Systems turns five. Journal of Unmanned Vehicle Systems 6:vi-xv.

Chabot, D., and D. M. Bird. 2012. Evaluation of an off-the-shelf unmanned aircraft system for surveying flocks of geese. Waterbirds 35:170–174. doi:10.1675/063.035.0119.

Chabot, D., and D. M. Bird. 2013. Small unmanned aircraft: Precise and convenient new tools for surveying wetlands. Journal Unmanned Vehicle Systems 1:15–24. doi: 10.1139/juvs-2013-0014.

Chrétien, L.-P., J. Théau, and P. Ménard. 2015. Wildlife multispecies remote sensing using visible and thermal infrared imagery acquired from an unmanned aerial vehicle (UAV). The International Archives of the Photogrammetry, Remote Sensing and Spatial Information Sciences XL-1/W4, 241–248.

Chrétien, L.-P., J. Théau, and P. Ménard. 2016. Visible and thermal infrared remote sensing for the detection of white-tailed deer using an unmanned aerial system. Wildlife Society Bulletin 40:181–191.

Christiansen, P., K. Steen, R. Jørgensen, and H. Karstoft. 2014. Automated detection and recognition of wildlife using thermal cameras. Sensors 14:13778–13793.

Cooch, E. (2008). Program MARK: A gentle introduction. Retrieved from http://www. phidot. org/software/mark/docs/book/

Croston, R., C. A. Hartman, M. P. Herzog, M. L. Casazza, C. L. Feldheim, J. T. Ackerman. 2020. Timing, frequency, and duration of incubation recesses in dabbling ducks. Ecology and evolution 10:2513–2529.

Custers, B. 2016. Drones here, there and everywhere introduction and overview. Pages 3–20 *in* B. Custers, editor. The Future of Drone Use. T.M.C. Asser Press, The Hague, The Netherlands.

Daubenmire, R. 1959. A canopy coverage method of vegetation analysis. Northwestern Science 33:43-65.

Davis, S. K. 2003. Nesting ecology of mixed-grass prairie songbirds in southern Saskatchewan. The Wilson Bulletin (Wilson Ornithological Society) 115:119–130. doi.org/10.1676/02-138.

Desante, D. F., and G. R. Geupel. 1987. Landbird productivity in central coastal California: the relationship to annual rainfall, and a reproductive failure in 1986. The Condor 89:636–653.

Doherty, K. E., D. W. Howerter, J. H. Devries, and J. Walker. 2018. Prairie Pothole Region of North America. Pages 679–688 *in* Finlayson, M. Everard, K. Irvine, R. J. McInnes, B. A. Middleton, A. A. van Dam, and N. C. Davidson, editors. The wetland book I: Structure and Function, Management, and Methods. Springer, Dordrecht, Dordrecht, The Netherlands

Duebbert, H. F., and H. A. Kantrud. 1974. Upland duck nesting related to land use and predator reduction. Journal of Wildlife Management 38:257–265.

Dumke, R. T., and C. M. Pils. 1979. Renesting and dynamics of nest site selection by Wisconsin pheasants. Journal of Wildlife Management 43:705–716.

Earl, J. P. 1950. Production of mallards on irrigated land in the Sacramento Valley, California. The Journal of Wildlife Management 14 :332-342.

Evans, R. D., and C. W. Wolfe, Jr. 1967. Effects of nest searching on fates of pheasant nests. Journal of Wildlife Management 31:754–759.

Galligan, E. W., G. S. Bakken, and S. L. Lima. 2003. Using a thermographic imager to find nests of grassland birds. Wildlife Society Bulletin 31:865–869.

Garner, D. L., H. B. Underwood, and W. F. Porter. 1995. Use of modern infrared thermography for wildlife population surveys. Environmental Management 19:233–238.

Gillette, G. L., P. S. Coates, S. Petersen, and J. P. Romero. 2013. Can reliable sage-grouse lek counts be obtained using aerial infrared technology? Journal of Fish and Wildlife Management 4:386–394.

Gloutney, M. L., R. G. Clark, A. D. Afton, and G. J. Huff. 1993. Timing of nest searches for upland nesting waterfowl. The Journal of Wildlife Management 57:597-601.

Glover, F. A. 1956. Nesting and production of the blue-winged teal (Anas discors Linnaeus) in northwest Iowa. The Journal of Wildlife Management 20:28– 46.

Gonzalez, L., G. Montes, E. Puig, S. Johnson, K. Mengersen, and K. Gaston. 2016. Unmanned aerial vehicles (UAVs) and artificial intelligence revolutionizing wildlife monitoring and conservation. Sensors 16:1–18.

Goosen, J. P. 1990. Prairie piping plover conservation: second annual report (1989). Unpublished Canadian Wildlife Service Report. Prairie Piping Plover Recovery Team. Edmonton, Canada.

Götmark, F. 1992. The effects of investigator disturbance on nesting birds. Current Ornithology 9:63–104.

Hardin, P. J., and M. W. Jackson. 2005. An unmanned aerial vehicle for rangeland photography. Rangeland Ecology and Management 58:439–442.

Havens, K. J., and E. J. Sharp. 2016. Thermal imaging techniques to survey and monitor animals in the wild. Academic Press, London, UK.

Helvey, M. W. 2020. Application of thermal and ultraviolet sensors in remote sensing of upland ducks. Thesis, Rochester Institute of Technology, Rochester, New York, USA.

Helvey, M., M. Ryckman, S. Ellis-Felege, J. Van Aardt and C. Salvagio. 2020*a*. Duck nest detection through remote sensing. Pages 6321–6324 *in* Proceedings of International Geoscience and Remote Sensing Symposium. IEEE Geoscience and Remote Sensing Society Symposium 2020, Waikoloa, HI, USA. doi:10.1109/IGARSS39084.2020.9323500.

Higgins, K. F., L. M. Kirsch, and I. J. Ball Jr. 1969. A cable-chain device for locating duck nests. The Journal of Wildlife Management 33:1009-1011.

Higgins, K. F., L. M. Kirsch, H. F. Duebbert, and A. Klett. 1977. Construction and operation of cable-chain drag for nest searches. U.S. Fish and Wildlife Service Resource Publication 512, Washington, D.C. USA.

Hodgson, J. C., and L. P. Koh. 2016. Best practice for minimizing unmanned aerial vehicle disturbance to wildlife in biological field research. Current Biology 26:R404–R405.

Hodgson, J. C., S. M. Baylis, R. Mott, A. Herrod, and R. H. Clarke. 2016*a*. Precision wildlife monitoring using unmanned aerial vehicles. Scientific Reports 6: 22574.

Hoekman, S. T., S. Mills, D. W. Howerter, J. H. Devries, I. J. Ball. 2002. Sensitivity analyses of the life cycle of midcontinent mallards. The Journal of Wildlife Management, 66:883–900.

Hovick, T. J., J. R. Miller, S. J. Dinsmore, D. M. Engle, D. M. Debinski, and S. D. Fuhlendorf. 2012. Effects of fire and grazing on grasshopper sparrow nest survival. The Journal of Wildlife Management 76:19–27.

Huggins R. M. 1991. Some practical aspects of a conditional likelihood approach to capture experiments. Biometrics 47:725–732.

Israel, M., and A. Reinhard. 2017. Detecting nests of lapwing birds with the aid of a small unmanned aerial vehicle with thermal camera. Pages 1199–1207 *in* proceedings of 2017 International Conference on Unmanned Aircraft Systems (ICUAS), Miami, FL, USA.

Johnson, E. W., and Ross, J. 2008. Quantifying error in aerial survey data. Australian Forestry 71:216–222.

Jones, H. 2004. Application of thermal imaging and infrared sensing in plant physiology and ecophysiology. Pages 107–163 *in* J. A. Callow, editor in chief. Advances in Botanical Research. Academic Press, Amsterdam, The Netherlands. doi.org/10.1016/S0065-2296(04)41003-9.

Jones , G. P., L. G. Pearlstine, and H. F. Percival. 2006 An assessment of small unmanned aerial vehicles for wildlife research. Wildlife Society Bulletin 34:750-758.

Kantrud, H. A., G. A. Swanson, G. L. Krapu, U.S. Fish and Wildlife Service Northern Prairie Wildlife Research Center. 1989. Prairie basin wetlands of the Dakotas: a community profile. U.S. Department of the Interior, Fish and Wildlife Service, Research and Development. Biological Report 85, Washington, DC, USA.

Keith, L. B. 1961. A study of waterfowl ecology on small impoundments in southeastern Alberta. Wildlife Monographs 6:3–88.

Kinzel, P. J., J. M. Nelson, R. S. Parker, and L. R. Davis. 2006. Spring census of mid-continent sandhill cranes using aerial infrared videography. The Journal of Wildlife Management 70:70–77.

Klett, A. T., H. F. Duebbert, C. A. Faanes, and K. F. Higgins. 1986. Techniques for Studying Nest Success in upland Habitats in the Prairie Pothole Region. U.S. Fish and Wildlife Service Resource Publication 158, Washington, D.C., USA.

Koh, L. P., and S. A. Wich. 2012. Dawn of drone ecology: low-cost autonomous aerial vehicles for conservation. Tropical conservation science, 5:121-132.

Koons, D. N., G. Gunnarsson, J. A. Schmutz, and J. J. Rotella. 2014. Drivers of waterfowl population dynamics: from teal to swans. Wildfowl 4:169-191.

Labisky, R. F. 1957. Relation of hay harvesting to duck nesting under a refuge-permittee system. The Journal of Wildlife Management 21:194–200.

Lawson, D. M., C. K. Williams, D. Howell, J. Fuller, and R. Stander. 2017. Coastal North Carolina American black duck breeding ecology study. University of Delaware Department of Entomology and Wildlife Ecology. <https://cdn.canr.udel.edu/wp-content/uploads/2017/09/20200021/Coastal-North-Carolina-American-Black-Duck-Nesting-Ecology-Study-2017-Field-Season-Report-colloquial.pdf>. Accessed 9 Feb 2018.

Lee, K. 2004. Development of unmanned aerial vehicle (uav) for wildlife surveillance. Dissertation, University of Florida, Florida, USA.

Lehmann, V. W. 1941. Attwater's prairie chicken its life history and management. North American Fauna 57:1–65.

Leon, A. M. 1997. Preliminary weight sizing and configuration layout for a small unmanned aerial vehicle (SUAV). Dissertation, Massachusetts Institute of Technology, Cambridge, Massachusetts, USA.

Lhoest, S., J. Linchant, S. Quevauvillers, C. Vermeulen, and P. Lejeune. 2015. How many hippos (HOMHIP): Algorithm for automatic counts of animals with infra-red thermal imagery from UAV. International Archives of the Photogrammetry, Remote Sensing and Spatial Information Sciences XL-3/W3, 355–362

Livezey, B. C. 1980. Effects of elected observer-related factors on fates of duck nests. Wildlife Society Bulletin 8:123–128.

Lloyd, P. and É. E. Plagányi. 2002. Correcting observer effect bias in estimates of nesting success of a coastal bird, the white-fronted plover *Charadrius marginatus*: A recently developed observer-effects model gives better estimates than the survival model. Bird Study 49:124–130.

Longmore, S. N., R. P. Collins, S. Pfeifer, S. E. Fox, M. Mulero-Pázmány, F. Bezombes, A. Goodwin, M. De Juan Ovelar, J. H. Knapen, and S. A. Wich. 2017. Adapting astronomical source detection software to help detect animals in thermal images obtained by unmanned aerial systems. International Journal of Remote Sensing 38:2623–2638.

Loos, E. R., and F. C. Rohwer. 2004. Laying-Stage Nest Attendance and Onset of Incubation in Prairie Nesting Ducks. The Auk, 12 (2), 587–599.

Mahoney, S. P., P. Krausman, and J. N. Weir. 2015. Challenges for conservation and sustainable use in North America. International Journal of Environmental Studies 72:879–886.

Martin, T. E., and G. R. Geupel. 1993. Nest-monitoring plots: methods for locating nests and monitoring success. Journal of Field Ornithology 64:507–519.

McCafferty, D. J. 2013. Applications of thermal imaging in avian science. Ibis 155:4–15.

Miller, H. W., and D. H. Johnson. 1978. Interpreting the Results of Nesting Studies. The Journal of Wildlife Management 423, 471–476. doi.org/10.2307/3800806.

Mills, W. E., D. E. Harrigal, S. F. Owen, W. F. Dukes, D. A. Barrineau, and E. P. Wiggers. 2011. Capturing clapper rails using thermal imaging technology. The Journal of Wildlife Management 75:1218–1221.

Montanaro, M., A. Gerace, A. Lunsford, and D. Reuter. 2014. Stray Light Artifacts in Imagery from the Landsat 8 Thermal Infrared Sensor. Remote Sensing 6:10435–10456. doi.org/10.3390/rs61110435.

Mulero-Pázmány, M., S. Jenni-Eiermann, N. Strebel, T. Sattler, J. J. Negro, and Z. Tablado. 2017. Unmanned aircraft systems as a new source of disturbance for wildlife: A systematic review. PLOS ONE 12:e0178448.

Murphy, R. K., B. G. Root, P. M. Mayer, J. P. Goossen, and K. A. Smith. 1999. A draft protocol for assessing piping plover reproductive success on Great Plains alkali lakes. Pages 90–107 *in* Proceedings of the 1998 Piping Plovers and Least Terns of the Great Plains and Nearby: A Symposium/Workshop., 2–5 February 1998, Omaha, NE. Edited by K. F. Higgins, M. R. Brashier, and C. D. Kruse. South Dakota State University, Brookings, USA.

National Oceanic and Atmospheric Administration (NOAA). 2022. <https://www.ncei.noaa.gov/>. Accessed 9 June 2022.

Quilter, M. C., and V. J. Anderson. 2000. Low altitude/large scale aerial photographs: a tool for range and resource managers. Rangelands 22:13–17.

R Core Team (2018). R: A language and environment for statistical computing. R Foundation for Statistical Computing, Vienna, Austria. URL https://www.R-project.org/.

Ralph, C. J., G. R. Geupel, P. Pyle, T. E. Martin, and D. F. DeSante. 1993. Handbook of field methods for monitoring landbirds. Director 144:1–41.

Rango, A., A. Laliberte, C. Steele, J. E. Herrick, B. Bestelmeyer, T. Schmugge, A. Roanhorse, and V. Jenkins. 2006. Using unmanned aerial vehicles for rangelands: current applications and future potentials. Environmental Practice 8:159–168.

Robel, R. J., J. N. Briggs, A. D. Dayton, and L. C. Hulbert. 1970. Relationships between visual obstruction measurements and weight of grassland vegetation. Journal of Range Management 23:295-297.

Santangeli, A., Y. Chen, E. Kluen, R. Chirumamilla, J. Tiainen, and J. Loehr. 2020. Integrating drone-borne thermal imaging with artificial intelligence to locate bird nests on agricultural land. Scientific reports. 10:1–8.

Schemlzeisen, R., D. R. C. Prescott, and L. Engley. 2004. Methods for controlling depredation on piping plovers in Alberta: a literature review and synthesis. Alberta Sustainable Resource Development, Fish and Wildlife Division, Alberta Species at Risk Report No. 84, Edmonton, Canada.

Scholten, C., A. Kamphuis, K. Vredevoogt, K. Lee-Strydhorst, J. Atma, C. Shea, O. Lamberg, and D. Proppe. 2019. Real-time thermal imagery from an unmanned aerial vehicle can locate ground nests of a grassland songbird at rates similar to traditional methods. Biological Conservation 233:241-246. doi.org/10.1016/j.biocon.2019.03.001.

Seymour, A. C., J. Dale, M. Hammill, P. N. Halpin, and D. W. Johnston. 2017. Automated detection and enumeration of marine wildlife using unmanned aircraft systems (UAS) and thermal imagery. Scientific Reports 7:45127.

Shewring, M. P. and J. O. Vafidis. 2021. Using UAV-mounted thermal cameras to detect the presence of nesting nightjar in upland clear-fell: A case study in South Wales, UK. Ecological Solutions and Evidence 2:e12052. doi.org/10.1002/2688-8319.12052.

SkyVector 2021. SkyVector Aeronautical Charts. <SkyVector: Flight Planning / Aeronautical Charts>. Accessed 17 May 2021.

Springer, P. J. 2013. Military robots and drones: a reference handbook. ABC-CLIO, Santa Barbara, California, USA.

Stackhouse, J. W., K. K. Sedivec, and B. A. Geaumont. 2013. Evaluation of three nest searching methods for ring-necked pheasant. Prairie Naturalist 45:114–117.

Stander, R., D. J. Walker, F. C. Rohwer, and R. K. Baydack. 2021. Drone nest searching applications using a thermal camera. Wildlife Society Bulletin 45: 371-382. doi.org/10.1002/wsb.1211.

Steel, P. E., P. D. Dalke, and E. G. Bizeau. 1956. Duck production at Gray's Lake, Idaho. The Journal of Wildlife Management 20: 279-285.

Strindberg, S., S. T. Buckland, and L. Thomas. 2004. Design of distance sampling surveys and geographic information systems. Pages 190–229 *in* Advanced Distance Sampling: Estimating Abundance of Biological Populations. Oxford University Press, Oxford, UK.

The Weather Company. 2022. Devils Lake, ND Weather History, May–June 2018. Weather Underground. <https://www.wunderground.com/history/monthly/us/nd/devils-lake/KDVL/date/>. Accessed 28 October 28, 2022.

Uhe, L., K. Albrecht, A. Schleicher, J. O. Engler. 2020. Adjusting trail cameras to improve monitoring of small open cup nesting birds. Journal of Ornithology 161:893–899. https://doi-org.uml.idm.oclc.org/10.1007/s10336-020-01758-9/

United States Fish and Wildlife Service. 2012. Thunderstorm Map for the Prairie Pothole Joint Venture. (GIS data shared by USFWS staff).

Vollmer, M. and K.-P. Möllmann. 2018. Infrared thermal imaging: fundamentals, research and applications. Second edition. Wiley-VCH, Weinheim, Germany.

Walker, J. W. 1993. Low altitude large scale reconnaissance : a method of obtaining high resolution vertical photographs for small areas. Interagency Archeological Services, Rocky Mountain Regional Office. National Park Service, Denver, Colorado, USA.

Watts, A. C., J. H. Perry, S. E. Smith, M. A. Burgess, B. E. Wilkinson, Z. Szantoi, P. G. Ifju, and H. F. Percival. 2010. Small unmanned aircraft systems for low-altitude aerial surveys. The Journal of Wildlife Management, 74: 1614–1619.

Weller, M. W. 1956. A Simple Field Candler for Waterfowl Eggs. The Journal of Wildlife Management 20:111.

White, G. C., and K. P. Burnham. 1999. Program MARK: survival estimation from populations of marked animals. Bird Study, 46(Supplement):s120–s138.

Whiteside, R. W., and F. S. Guthery. 1983. Ring-necked pheasant movements, home ranges, and habitat use in west Texas. The Journal of Wildlife Management 47:1097–1104.

Williams, B., M. Koneff, and D. A. Smith. 1999. Evaluation of Waterfowl Conservation under the North American Waterfowl Management Plan. The Journal of Wildlife Management, 63:417–440. doi.org/10.2307/3802628